UNIVERSITY OF CALIFORNIA, SAN DIEGO

The Role of IL-17D in Immunosurveillance

A dissertation submitted in partial satisfaction of the

requirements for the degree Doctor of Philiosophy

in

Neurosciences

by

Robert Saddawi-Konefka

Committee in charge:

Professor Jack Bui, Chair
Professor John Chang
Professor John Crawford
Professor Subhojit Roy
Professor Ajit Varki

2015

The Dissertation of Robert Saddawi-Konefka is approved, and is acceptable

In quality and form for publication on microfilm and electronically:

_____

_____

_____

_____

_____

Chair

University of California, San Diego

2015

DEDICATION

In recognition of all she teaches me and how she inspires me this dissertation is dedicated to my daughter Juna Saddawi-Banno.

EPIGRAPH

"The closer you get to real matter, rock air fire and wood…the more spiritual the world is."

Jack Kerouac

TABLE OF CONTENTS

LIST OF FIGURES

LIST OF TABLES

ACKNOWLEDGEMENTS

I would like to acknowledge Professor Jack Bui for his support as the chair of my committee. I thank Dr. Bui teaching me by example: mentoring me with his level-headed approach in the lab, his contagious excitement for science and his laser-quick insight.

I would like to acknowledge Dr. Timothy O'Sullivan for his support and friendship. I thank Tim for the long, lonely days we spent sorting macrophages, the lunch breaks, and the years we spent together experimenting.

I would like to acknowledge Dr. Asoka Banno and Juna Saddawi-Banno for their support and love. Going to lab everyday is only fun when I can come home to you two.

Chapter 1, in full, is an adapted version of material as it appears in The Journal of Experimental Medicine, 2012, Saddawi-Konefka, Robert; Smyth Mark J.; Schreiber, Robert D.; Bui, Jack D.; The Rockefeller University Press. The disseration author was the primary co-author of this paper.

Chapter 2, in full, is an adapted version of the material as it appears in Cell Reports, 2014, Timothy O'Sullivan, William Vermi, Catherine M Koebel, Cora Arthur, J Michael White, Ravi Uppaluri, Daniel M Andrews, Shin Foong Ngiow, Michele W L Teng, Mark J Smyth, Robert D Schreiber, and Jack D Bui; Elsevier Ltd. The dissertation author was the second author of this paper.

Chapter 3, in part, is an adapted version of material that is currently being prepared for submission for publication. Saddawi-Konefka, Robert; Bui, Jack D.; Mayfield, Stephen P.; Tran, Miller. The dissertation author was the primary author of this material.

VITA

2008 Bachelor of Arts, University of Southern California

2015 Doctor of Philosophy, University of California, San Diego

PUBLICATIONS

Robert Saddawi-Konefka, Ruth Seelige, Emilie T.E. Gross, Stephen C. Searles, Allen Jr. Washington, Endi K. Santosa, Beichen Liu, Calvin Duong, Timothy E. O'Sullivan, Jack D. Bui. Nrf2 induces IL-17D to mediate tumor and virus surveillance. *in submission* (2015)

Robert Saddawi-Konefka, O'Sullivan, T., Gross, E. T., Washington, A., Jr & Bui, J. D. Tumor-expressed IL-17D recruits NK cells to reject tumors. *Oncoimmunology* 3, e954853 (2015).

Timothy O'Sullivan, **Robert Saddawi-Konefka**, Emilie Gross, Miller Tran, Stephen P Mayfield, Jack D Bui. Interleukin-17D Mediates Tumor Rejection through Recruitment of Natural Killer Cells. *Cell Reports* 7, 989–998 (2014).

Robert Saddawi-Konefka, Timothy O'Sullivan, William Vermi, Catherine M Koebel, Cora Arthur, J Michael White, Ravi Uppaluri, Daniel M Andrews, Shin Foong Ngiow, Michele W L Teng, Mark J Smyth, Robert D Schreiber, and Jack D Bui. Cancer immunoediting by the innate immune system in the absence of adaptive immunity. *Journal of Experimental Medicine* 209, 1869–1882 (2012).

Robert Saddawi-Konefka & Crawford, J. R. Chronic viral infection and primary central nervous system malignancy. *J Neuroimmune Pharmacol* 5, 387–403 (2010).

FIELDS OF STUDY

Major Field: Immunology

Studies in Tumor Immunology
Professor Jack Bui

ABSTRACT OF THE DISSERTATION

The Role of IL-17D in Immunesurveillance

by

Robert Saddawi-Konefka

Doctor of Philosophy in Neurosciences

University of California, San Diego, 2015

Professor Jack Bui, Chair

The pathology of malignancy and viral infection force cells into the "stressed state," characterized by altered metabolism and imbalanced reactive oxidative species (ROS) [1-3]. This generalized state of cellular stress engenders a protective surveillance response by the host immune system[4-11]. Under homeostatic conditions, the immune

surveillance of stressed cells leads to their destruction; and, thus, many stressed cells experience tremendous selective pressure to develop immune-evasive programs[5-8,12]. Targeting these immune evasive programs in stressed cells as well as identifying the signaling pathways and molecules that influence surveillance have been a top priority[13-15]. We hypothesize that stressed cell-expressed factors can influence the nature and activity of immune cells, thereby determining whether tumors and viral infections progress. To address this central hypothesis, we have endeavored to: First, define how the immune system influences tumor development and progression; Second, explore which signals can recruit immune cells into tumors; and, Third, to determine how cellular stress inherent to malignancy or viral infection induce immune-cell recruiting signals to initiate immunosurveillance.

CHAPTER 1: CANCER IMMUNOEDITING BY THE INNATE IMMUNE SYSTEM

Immune cells can infiltrate a developing tumor mass and either promote or inhibit tumorigenesis [7,16,17]. Cancer immunoediting describes the process whereby the interaction between immune cells and tumor cells either eliminates the developing tumor, holds it in a state of growth dormancy, or generates a tumor cell repertoire that is capable of survival in immune-competent hosts[18-20]. Several studies have revealed the contribution of adaptive and innate immunity in cancer immunoediting[18,19,21-27], but it is not clear whether the unmanipulated innate immune system can suppress tumor formation without adaptive immunity.

We hypothesize that the innate immune system can control tumor formation in the absence of adaptive immunity. It has been shown that natural killer cells (NK;[6,28] and classically activated M1 macrophages[29,30] support a Th1 response that can ultimately lead to tumor rejection in the presence of adaptive immunity, but it is not clear whether these cells interact in the absence of adaptive immunity to suppress tumor formation in primary tumor models. In contrast, other studies have found that the innate immune system can promote tumor formation via alternatively activated M2 macrophages[31] that augment angiogenesis and promote tissue invasion. M2 macrophages also inhibit the formation of antitumor adaptive immunity, and therefore it is possible that innate immunity would promote tumor formation in the absence of adaptive immunity. Using the 3-MethylCholanthrene (MCA) model of sarcomagenesis, we found both increased incidence and immunogenicity of MCA- induced sarcomas in *rag2*$^{-/-}$ x $\gamma c^{-/-}$ mice

compared with *rag2*$^{-/-}$ mice, which, consistent with previous results[18] had increased incidence and immunogenicity of tumors compared with WT mice. When transplanted into *rag2*$^{-/-}$ recipients, rag*2*$^{-/-}$ x γ*c*$^{-/-}$ regressor sarcoma cell lines formed tumors that became heavily infiltrated with M1 macrophages. The infiltration of M1 macrophages was associated with tumor editing and required host γc and IFN-γ activity. In contrast, in the absence of γc and IFN-γ function, *rag2*$^{-/-}$ x *γc*$^{-/-}$ regressors were infiltrated with more M2 macrophages, which can promote tumor formation[29]. We also found that M1 macrophages can be elicited by CD40 agonistic antibodies to restore the editing capacity of *rag2*$^{-/-}$x *gc*$^{-/-}$mice. These studies document that components of the innate immune system present in *rag2*$^{-/-}$ mice can manifest certain types of cancer immunoediting capacity in the absence of adaptive immunity and point, specifically, to M1 macrophages as important effectors in this process.

MCA-induced sarcoma incidence is increased in *rag2*$^{-/-}$x *γc*$^{-/-}$ mice compared to syngeneic *rag2*$^{-/-}$ and WT mice.

To determine whether the innate immune system of *rag2*$^{-/-}$ mice was capable of tumor immunosurveillance, we compared the incidence of MCA-induced sarcomas in immunologically intact WT C57BL/6 mice to that of C57BL/6 mice with defects in either adaptive immunity only (*rag2*$^{-/-}$ mice) or in both adaptive and innate immunity (*rag2*$^{-/-}$ x γc$^{-/-}$ mice). Figure 1.1 shows that the incidence of sarcomas was higher in *rag2*$^{-/-}$ x γc$^{-/-}$ mice compared to RAG2$^{-/-}$ mice at all doses tested. In addition, at MCA doses of 25 μg or 100 μg, *rag2*$^{-/-}$x γc$^{-/-}$ mice developed sarcomas slightly faster than *rag2*$^{-/-}$ mice, indicating

that the innate immune system in *rag2*$^{-/-}$ mice controlled MCA-induced tumor outgrowth to some extent.

Growth of MCA-induced sarcoma cell lines derived from RAG2$^{-/-}$ x γc$^{-/-}$ mice is inhibited when transplanted into syngeneic WT mice.

To study tumor editing, low passage cell lines were derived from primary MCA tumor masses generated in C57BL/6 WT, *rag2*$^{-/-}$, and *rag2*$^{-/-}$x γc$^{-/-}$ mice, and the immunogenicity of each cell line was assessed by transplanting them into naïve WT syngeneic mice and monitoring their growth. As described previously, we observed two divergent growth phenotypes among the transplanted sarcomas: a regressor phenotype, defined by a failure to form a mass of >9 mm in diameter in more than 50% of transplantations into syngeneic WT mice, and a progressor phenotype, defined by the formation of masses >9 mm in more than 50% of transplantations into WT mice. When we examined groups of MCA-induced sarcoma cell lines generated from WT, *rag2*$^{-/-}$, and *rag2*$^{-/-}$x γc$^{-/-}$ mice, we found that the proportion of regressor MCA-induced sarcoma cell lines was 0/9 WT, 3/10 *rag2*$^{-/-}$, and 6/10 *rag2*$^{-/-}$x gc$^{-/-}$ (Fig. 1.2 A, right panels). All cell lines grew when transplanted into *rag2*$^{-/-}$ mice (Fig. 1.2 A, left panels), indicating that their rejection was due to the adaptive immune system and was not simply a failure to grow in vivo.

To determine the overall immunogenicity of each group of tumors, we examined the tumor-free survival of large cohorts of WT and *rag2*$^{-/-}$ mice challenged with panels of tumor cell lines derived from WT, *rag2*$^{-/-}$, or *rag2*$^{-/-}$x γc$^{-/-}$ mice (Fig. 1.2 B). All MCA-

induced sarcoma cell lines formed tumors in RAG2$^{-/-}$ mice by 36 days post-tumor cell transplant (data not shown). In contrast, the kinetics and frequency of tumor formation in WT recipients was dependent upon the level of immune function of the original source from which the tumor cells were derived. Specifically, when 17 tumor cell lines derived from *rag2*$^{-/-}$x γc$^{-/-}$ mice were transplanted into a total of 132 naïve, syngeneic WT mice, only 46% of the mice formed tumors by 70 days post-transplant (Fig. 1.2 B, $p < 0.001$ for all comparisons). Over a similar time course, MCA-induced sarcoma cell lines from 15 RAG2$^{-/-}$ and 9 WT mice formed tumors in 64% and 97% of WT recipients, respectively. These results were reproduced in an independent MCA induction experiment, and the combined results of these two experiments, encompassing 71 total MCA-induced sarcoma cell lines transplanted into 474 WT mice, 94 *rag2*$^{-/-}$ mice, or 51 *rag2*$^{-/-}$x γc$^{-/-}$ mice, are shown in Table 1. Altogether, these results support the hypothesis that tumors from mice with greater immunodeficiency undergo decreased levels of immunoediting.

Tumor cell lines generated in *rag2*$^{-/-}$x γc$^{-/-}$ mice show an increased regressor frequency compared to cell lines from WT and *rag2*$^{-/-}$ mice.

Previous work has shown that the percentage of regressors within a group of MCA-induced sarcoma cell lines, the "regressor frequency" was 40% when the MCA-induced sarcoma cell lines were generated in *rag2*$^{-/-}$ mice and 0% when the cell lines were generated in WT mice. These percentages are remarkably reproducible and have remained so even when experiments have been conducted in our three independent

laboratories in La Jolla, St. Louis, and Melbourne (Fig. 1.3). Specifically, we found a consistent regressor frequency of 0% when MCA-induced sarcoma cell lines are generated in WT mice (50 cell lines from two strains and four independent experiments). Notably, MCA-induced sarcoma cell lines derived from *rag2*$^{-/-}$ mice displayed a 30-44% regressor frequency (82 cell lines from three strains and four independent experiments). MCA-induced sarcoma cell lines derived from *rag2*$^{-/-}$ x γc$^{-/-}$ mice had the highest regressor frequency (60-70%), indicating that as a group, these cell lines were the most immunogenic and least edited.

rag2$^{-/-}$x γc$^{-/-}$ regressors undergo editing when transplanted into _rag2_$^{-/-}$ mice.

Since regressor cell lines generated from *rag2*$^{-/-}$x γc$^{-/-}$ mice displayed the highest levels of immunogenicity and, subsequently, the lowest levels of immunoediting compared to *rag2*$^{-/-}$ and WT mice, we hypothesized that the innate immune system of *rag2*$^{-/-}$ mice could edit these tumor cell lines in vivo. We tested this by transplanting two independent sarcoma cell lines generated from *rag2*$^{-/-}$x γc$^{-/-}$ mice into either *rag2*$^{-/-}$ or *rag2*$^{-/-}$x γc$^{-/-}$ mice. To determine if in vivo passaging altered the immunogenicity of these cell lines, tumor masses were harvested at day 25 and converted into cell lines. When these cell lines were transplanted into WT mice, 88% of *rag2*$^{-/-}$-passaged tumor cell lines formed progressively growing tumor masses by day 40 compared to 46% of *rag2*$^{-/-}$x γc$^{-/-}$-passaged and 10% of unpassaged cell lines (Fig. 1.4 A, $p = 0.025$). These results suggest a higher level of editing by the innate immune system in *rag2*$^{-/-}$ versus *rag2*$^{-/-}$x γc$^{-/-}$ mice

but also indicate that there is some level of measurable tumor sculpting in *rag2*$^{-/-}$x γc$^{-/-}$ mice, which could be due to residual immune function or a non-immunologic editing process.

NK cells do not preferentially kill regressor versus progressor tumor cells.

Having shown that γc is important for the ability of innate immunity to control and edit MCA-induced sarcomas, we predicted that NK cells, dependent upon γc for development[32], would participate in this editing process in vivo. To explore whether NK cells preferentially recognize regressors over progressors, we performed standard chromium release cytotoxicity assays[33] and also examined the NK cell content in regressor versus progressor tumors. We found that the overall susceptibility to NK cell killing of 10 MCA-induced sarcoma cell lines from *rag2*$^{-/-}$x γc$^{-/-}$ mice did not differ from that of 10 MCA-induced sarcoma cell lines from *rag2*$^{-/-}$, or 9 MCA-induced sarcomas from WT mice (Fig. 1.4 B). Even when all tumors were grouped based on phenotypic growth in WT mice – grouped into progressors or regressors – we observed no difference in NK cell-specific lysis (Fig. 1.4 B). Additionally, we did not detect a difference in NK1.1^{+} cell infiltration (approximately 5%) into any of the MCA-induced sarcomas after they were transplanted into *rag2*$^{-/-}$ mice (Fig. 1.4 C).

MHC class II positive macrophages are selectively present in regressor tumors during immunoediting.

We therefore re-directed our focus on myeloid cells as they represent the major hematopoietic lineage cell type that infiltrates either rejecting or progressively growing tumors[30]. To examine this issue, two *rag2*$^{-/-}$x γc$^{-/-}$ regressor cell lines were transplanted into either *rag2*$^{-/-}$ or *rag2*$^{-/-}$x γc$^{-/-}$ hosts, and tumors were harvested at day 15 and analyzed by immunohistochemistry to assess the number and phenotypes of infiltrating myeloid cells. No differences were detected in the total number of CD68^{+} macrophages infiltrating tumors growing in either *rag2*$^{-/-}$ or *rag*2$^{-/-}$x γc$^{-/-}$ hosts (Fig. 1.5 B, right panels). In contrast, we observed significantly higher numbers of MHC class II positive cells in tumors growing in *rag*2$^{-/-}$ versus *rag2*$^{-/-}$ x γc$^{-/-}$ hosts (Fig. 1.5 A, B, p = 0.00156, 0.0071). A similar preferential accumulation of MHC class II positive cells was also observed in unedited versus edited tumors growing in *rag*2$^{-/-}$ mice (Fig. 1.5 C,D,E).

Editing of regressor tumor cells from *rag*2$^{-/-}$x yc$^{-/-}$ mice and induction of MHC class II on tumor infiltrating cells requires NK cells and IFNγ production in vivo.

Since γc was important for editing, but NK cell-dependent tumor cell killing was not, we hypothesized that NK cell-derived IFNγ was critical for the editing process we observed in *rag*2$^{-/-}$ mice. We therefore transplanted a regressor cell line derived from a *rag*2$^{-/-}$x γc$^{-/-}$ mouse into *rag*2$^{-/-}$ recipients treated either with the neutralizing H22 IFNγ-specific monoclonal antibody (mAb), a NK1.1 specific monoclonal antibody (PK136), or a control mAb (PIP). Tumors were harvested at day 20 and converted into cell lines, which were subsequently transplanted into naïve, syngeneic WT hosts to measure tumor

free survival. We observed a statistically significant increase in the survival of WT mice transplanted with MCA-induced sarcomas that had been passaged through NK cell depleted and IFNγ-neutralized mice versus control mice (Fig. 1.6 A,B $p = 0.0042$, 0.0016), indicating that NK cells and IFNγ plays a critical role in activating the editing capacity of the innate immune system in *rag*$2^{-/-}$ mice. Analysis of tumor cross sections by immunohistochemistry at day 20 showed MHC class II positive macrophages were significantly reduced with anti-IFNγ treatment (Fig. 1.6 C,D, $p = 0.0432$), even though total macrophage infiltration did not differ between hosts as determined by $CD68^+$ events (Fig. 1.6 D). These results demonstrate that NK cells and IFNγ may facilitate editing by activating macrophages.

Tumor-associated macrophages (TAMs) from regressor tumors display an M1 phenotype and require NK cells and IFNγ for polarization in vivo.

Since the MHC class II^+ macrophages required IFNγ for their accumulation, we hypothesized that these macrophages were classically activated M1 macrophages and next performed immunophenotyping to detect the presence of tumor associated M1 or M2 macrophages, known to have anti- or pro-tumor functions, respectively[31,34]. For this purpose, we used a combination of IHC and FACS analysis combined with defining cytokine production in freshly harvested tumors. In all cases, we analyzed no fewer than three tumors across at least two experiments. We first performed IHC analysis for the M2-type macrophage marker CD206 and compared the staining pattern to that of MHC

class II (known to be upregulated on M1 macrophages versus M2 macrophages) (Fig. 1.7 A). We found that regressor tumors harvested from *rag*2$^{-/-}$ mice had the highest percentage of class II high events (29%) and lowest percentage of CD206^{+} events (33%). In contrast, tumors harvested from both *rag*2$^{-/-}$ mice depleted of IFNγ or *rag*2$^{-/-}$x γc$^{-/-}$ mice had significantly lower percentages of class II events (12% and 10%, respectively) and significantly higher percentages of CD206^{+} events (60% and 70%, respectively) (Fig. 1.7 A). Thus, IHC analysis suggested that M1-phenotype macrophage accumulation within tumors requires both IFNγ and γc. We next used FACS analysis to gate on TAM subsets using combinations of CD11b, Ly6C, and MHC class II to differentiate between M1 and M2 macrophages (Fig. 1.7 C) as previously described[35]. This gating strategy identified M1 macrophages as MHC class II^{hi}, Ly6C^{lo}, CD206^{lo}, F4/80^{hi} cells and M2 macrophages as MHC class II^{lo}, Ly6C^{lo}, CD206^{hi}, F4/80^{hi} cells (Fig. 1.7 C, D). This analysis showed that regressor tumors contained significantly higher percentages of M1 macrophages when isolated from *rag*2$^{-/-}$ mice treated with control mAb PIP (56%) compared to either *rag*2$^{-/-}$ mice treated with anti-NK1.1 mAb (28%), neutralizing IFNg mAb (37%), or *rag*2$^{-/-}$ x γc$^{-/-}$ (20%) mice (Fig. 1.7 B, top panel, $p < 0.0001$ for all populations). Conversely, M2 macrophage percentages were slightly increased in tumors isolated from *rag*2$^{-/-}$ mice treated with anti-IFNγ (36%) and *rag*2$^{-/-}$x γc$^{-/-}$ mice (37%), but not anti-NK1.1 treated mice (27%) compared to control *rag*2$^{-/-}$ mice (28%) (Fig. 1.7 B, bottom panel, $p = 0.0007$, 0.002 respectively), confirming our IHC results. Tumor cell suspensions isolated from the different groups of mice did not show differences in total numbers of CD45^{+} or CD11b^{+} cells (data not shown), thus ruling out the possibility that

the differences observed in TAM subsets were due to differential recruitment of immune cells in mice lacking either IFNy or γc function.

To test a functional marker of TAM polarization, we examined supernatant of matched tumor cell suspensions cultured in vitro. Cell suspensions from tumors growing in control *rag*$2^{-/-}$ mice contained high levels of IL-1a and IFNγ and produced levels of IL-6 and TNF that were similar to bone marrow-derived macrophages stimulated with LPS and IFNγ, indicative of a classically activated M1 macrophage cytokine profile. In contrast, cell suspensions derived from tumors derived from anti-IFNγ-treated *rag*$2^{-/-}$ mice and *rag*$2^{-/-}$ x $\gamma c^{-/-}$ mice produced significantly lower levels of each cytokine (Fig. 1.7 E, $p < 0.0001$ for all comparisons). We did not detect IL-10 or IL-4 production in any of the cultures, indicating that the M2 TAMs are not identical to alternatively activated M2 macrophages found in certain infections. No cytokine production was observed in cultures of the tumor cell line alone (data not shown). These results demonstrates that the cytokines that were detected in the cell suspensions derived from in vivo growing tumors can be attributed to the immune subsets that infiltrate the tumor. To further characterize TAM subsets in our midel we sorted M1 and M2 macrophages from regressor tumor cell suspensions derived from *rag2*$^{-/-}$ hosts to confirm their differentiation by qPCR. Sorted M1 TAMs contained higher transcript levels of classically activated macrophage genes TNf-a and iNOS, while containing less M2 specific genes arginase, eCAD, and GAS3 (Fig. 1.7F).

Polarization of M1 macrophages in vivo by administration of a CD40 agonist induces editing in *rag*2$^{-/-}$x γc$^{-/-}$ mice.

CD40 agonist administration in vivo has been shown to have anti-tumor properties[36,37] by activating TAMs to become tumoristatic through production of nitric oxide (NO)[38]. We hypothesized that CD40 agonist treatment would activate macrophages in tumors growing in *rag*2$^{-/-}$x γc$^{-/-}$ mice, thereby leading to editing of cancer cells in vivo. In order to test this, a regressor cell line was transplanted into *rag*2$^{-/-}$x γc$^{-/-}$ mice receiving a single injection of either control IgG or anti-CD40 agonist monoclonal antibodies, tumor masses were harvested, and cell lines were generated and transplanted into WT mice. We found that cell lines from CD40 agonist treated *rag2*$^{-/-}$x γc$^{-/-}$ mice formed tumor masses in 100% of WT recipients, whereas cell lines from isotype-treated *rag*2$^{-/-}$x γc$^{-/-}$ mice formed tumors in 33% of WT recipients in *rag*2$^{-/-}$x γc$^{-/-}$ mice (Fig. 1.8 A, $p = 0.0009$). We then analyzed the quantity of M1 macrophages in harvested tumor cell suspensions and found that M1 macrophage percentages were doubled in mice treated with CD40 agonist (36%) compared to control treatment (18%) (Fig. 1.8 B, upper panel, $p = 0.0003$). Correspondingly, M2 macrophages were decreased (23% vs 15%) by anti-CD40 agonist treatment (Fig. 1.8 B, lower panel, $p=0.0151$). These results suggest that TAMs can be activated in *rag2*$^{-/-}$x γc$^{-/-}$ mice to effectively edit tumors in vivo.

DISCUSSION

The cancer immunoediting hypothesis predicts that tumors arising in immune-deficient individuals will be more immunogenic than tumors that develop in immune-competent individuals. Although this concept is achieving wide acceptance, the relationship between the degree of host immune deficiency and the extent of cancer immunoediting have not yet been examined. In this study, we provide evidence that the extent of host immune-deficiency directly correlates with the level of cancer immunoediting. In doing so, we document that the innate immune system present in *rag2*$^{-/-}$ mice can mediate to some extent the immunosurveillance and immunoediting of MCA-induced sarcomas. This editing activity is associated with M1 macrophages, IFNg, gc, and NK cells.

Consistent with our previous studies[18,39], we found that tumors arising in *rag*-deficient mice are unedited and as a group, more immunogenic. Our evidence is based on studies of over 150 cell lines generated during a decade of experimentation performed in two separate sites, across two strains of mice, and using both *rag1*- and *rag2*-deficient models. A striking finding from our studies is that the regressor frequency of MCA-induced sarcoma cell lines derived from *rag*-deficient mice reproducibly approximates 40%. Moreover, the regressor frequency of MCA-induced sarcomas generated in mice lacking *rag* and gc is 60-70% in two independent experiments. These results suggest a quantitative nature to the immunoediting process, whereby a certain degree of basal immune function is associated with quantifiable levels of tumor sculpting, which can be measured by the regressor frequency. Since a majority of MCA cell lines generated from

rag2$^{-/-}$x γc$^{-/-}$ mice are regressors, we speculate that the primary tumor cell repertoire consists of mostly immunogenic tumor cells that are immunologically heterogeneous[38]. This heterogeneity can be partially sculpted by innate immunity in *rag*2$^{-/-}$ mice or fully sculpted by the complete immune system in WT mice. It should be noted that we have never been able to isolate regressors from MCA-induced sarcomas that develop in WT mice (regressor frequency of 0% of 50 cell lines). These results confirm that cancer immunoediting of MCA-induced sarcomas is quite robust in WT mice and further validate that immune escape is an essential hallmark of cancer cells[40].

We have provided evidence that the innate immune system can edit tumors and point to M1 macrophages as participants in this process. M1 macrophages are activated classically via IFNg and function in the removal of intracellular pathogens[31]. In the context of cancer, M1 macrophages can promote tumor elimination via activation of Th1 pathways and secretion of tumoricidal levels of nitric oxide[29]. In our studies, we have defined CD45^{+}CD11b^{+}MHC class II^{hi}CD206^{lo}Ly6C^{lo} cells as M1 macrophages based not only on their phenotype but also on their classical requirement for IFNg for their generation. Using this definition, we found a striking correlation between the presence of M1 macrophages and productive immune responses to regressor tumors. The administration of reagents that increased M1 percentages, such as CD40 agonist, enhanced editing, whereas treatments that decreased M1 percentages, such as NK cell depletion and anti-IFNg mAb blocked editing.

Our findings support an anti-tumor function for macrophages that is consistent with studies performed almost forty years ago, when it was shown that activated macrophages from infected mice[41]could kill syngeneic transformed murine embryonic

fibroblasts (MEFs) but not primary non-transformed MEFs[42] in vitro. This tumoricidal activity of macrophages required cell-cell contact and was induced largely by the cytokine IFNγ[43,44] in combination with additional signals such as lipopolysaccacharide (LPS)[45] or muramyl dipeptide[46]. Although we have not shown that regressor tumor cells are killed by TAMs, we have observed that regressor tumor cells can be killed effectively by IFNg-stimulated bone marrow macrophages *in vitro* (data not shown). Our attempts to demonstrate the tumoricidal activity of regressor-associated macrophages was limited by the poor viability of sorted TAMs. Furthermore, the requirement of macrophages in immunoediting could not be tested, as treatment with clodronate encapsulated liposomes failed to deplete macrophages in tumors, even though depletion of $CD11b^{+}$ macrophages was achieved in the spleens of tumor bearing mice (data not shown). Nevertheless, we favor the interpretation that M1 macrophages are the most likely editor in mice that lack adaptive cells given their abundance in the tumor, their enhanced presence in response to IFNg and NK cell activity, and their known tumoricidal activity.

Recent studies indicate that macrophage tumoricidal activity could be enhanced *in vitro* and *in vivo* upon administration of CD40 agonistic antibodies[35,36,47]. Notably, Beatty *et al.* investigated the role of tumoricidal macrophages activated in vivo with CD40 agonist treatments in the rejection of pancreatic ductal adenocarcinoma (PDA). After demonstrating the efficacy of the anti-CD40 agonist mAb CP-870,893 in human patients, the authors employed a mouse model of PDA to investigate the mechanism of tumor rejection with CD40 agonist treatment. To their surprise, the results indicated that CD40-stimulated macrophages, independent of T-cell activity, are sufficient to mediate PDA rejection in vivo. Similarly, we have found that CD40 agonist treatment of *rag*$2^{-/-}$x

$\gamma c^{-/-}$ mice can induce tumor editing in the absence of adaptive immunity and NK cells, thereby suggesting that macrophages are sufficient for tumor editing. In contrast to the Beatty study, we did not see tumor rejection, suggesting that MCA sarcomas require adaptive cells for their regression. Our studies also show that unmanipulated macrophages are capable of editing through IFNg and NK cells without the use of CD40 agonists.

We found that the accumulation of M1 macrophages in regressor tumors required IFNg and NK cells. The participation of NK cells in immunosurveillance against certain types of tumors has been clearly documented in studies showing increased tumor incidences in mice lacking NK cells or molecules associated with NK cell recognition or effector function[6,21,28], such as NKp46[48], NKG2D[49], DNAM-1[50,51], perforin[52,53], IFNγ[52], or TRAIL[54]. Therefore, we considered the possibility that there might be increased NK cell killing of MCA-induced sarcoma cells from *rag2*$^{-/-}$x $\gamma c^{-/-}$ versus *rag2*$^{-/-}$ or WT mice. However, we did not find major differences in the susceptibility of unedited versus edited tumors to NK cell killing. These results are consistent with recent studies showing that NKG2D, an activating receptor on NK cells that mediates tumor recognition and killing, did not play a role in the surveillance of MCA-induced sarcomas[49]. In this study, NKG2D-deficient mice had similar incidences of MCA-induced sarcomas but were more susceptible to tumor formation in prostate cancer and B lymphoma model systems, suggesting that the role of NK cells in destroying tumor cells could be dependent on the site of tumor formation. For MCA-induced sarcomas, we advocate that one role of NK cells in eliminating and/or sculpting tumors in the absence of adaptive immunity may be as a source of IFNg. This is based on findings that NK cells and IFNg are necessary for

M1 macrophage polarization and subsequent editing in *rag2*$^{-/-}$ mice. Although we cannot rule out the contribution of myeloid populations in IFNg production, sorted M1 and M2 TAMs do not show any IFNg transcript (data not shown), suggesting that NK cells are the predominant producers of IFNg in the *rag2*$^{-/-}$ host. It is not known what induces IFNg production by NK cells in our system, but our preliminary studies indicate that MCA-induced sarcoma cells are incapable of directly eliciting IFNg production from NK cells in vitro. Interestingly, IL-12p40 was shown to be required for MCA sarcoma surveillance[55], so it is possible that local IL-12 production could stimulate NK cells to produce IFNg to mediate editing in the absence of adaptive immunity. It should be noted that in *rag2*$^{-/-}$x γc$^{-/-}$ mice lacking NK cells, editing could be restored with CD40 agonist treatment, suggesting that direct interaction between NK cells and tumor cells is not needed for tumor editing – as long as M1 macrophages are present.

Our model is based on the postulate that immunogenic regressors, in the presence of M1 macrophages, are converted into non-immunogenic progressors, but we have not identified the molecular basis of this phenotypic conversion. Recent studies have also found that certain tumor cells can evade macrophage killing/phagocytosis by expressing high levels of CD47[56,57] and/or low levels of calreticulin[58]. Other studies have implicated calreticulin exposure as a key initiator of innate immune responses to tumor cells, leading to antigen presentation and productive adaptive anti-tumor responses, and the blockade of these pathways could be a mechanism of tumor escape[59]. We did not find differences in the interaction between bone marrow-derived macrophages and regressor versus progressor tumor cells in vitro (RSK, TEO, JDB, unpublished observations). Furthermore, our preliminary studies indicate that CD47 and calreticulin are not different between

regressor and progressor cells in vitro. Future studies will compare the gene expression profiles of regressor and progressor cells to identify pathways that may mediate innate cell recognition/editing. Our matched regressor/passaged-regressor cells will be critical for these experiments.

In summary, we document the generation and initial characterization of a novel set of unedited MCA-induced sarcoma cell lines that may be highly stimulatory for the innate immune system. The enhanced accumulation of M1 macrophages in these highly immunogenic tumors suggests that they can serve as models to study the early events that lead to the generation of M1 macrophages in regressing tumors. We also show that the innate immune system in *rag2*$^{-/-}$ mice contains sufficient cellular machinery to perform sculpting of MCA-induced sarcomas. This cellular machinery includes NK cells that produce IFNg to activate macrophages to function as innate editors. This cascade can lead to tumor elimination in the presence of adaptive immunity and/or editing in the absence of adaptive immunity. Finally, we introduce a quantitative dimension to the sculpting phase of cancer immunoediting by showing that the percentage of regressor cell lines generated from MCA-induced sarcomas is reproducible and correlates with the level of immune pressure in the tumor-bearing host.

Chapter 1, in full, is an adapted version of the material as it appears in The Journal of Experimental Medicine, 2012, O'Sullivan, Timothy; Smyth Mark J.; Schreiber, Robert D.; Bui, Jack D.; The Rockefeller University Press. The disseration author was the first co-author of this paper.

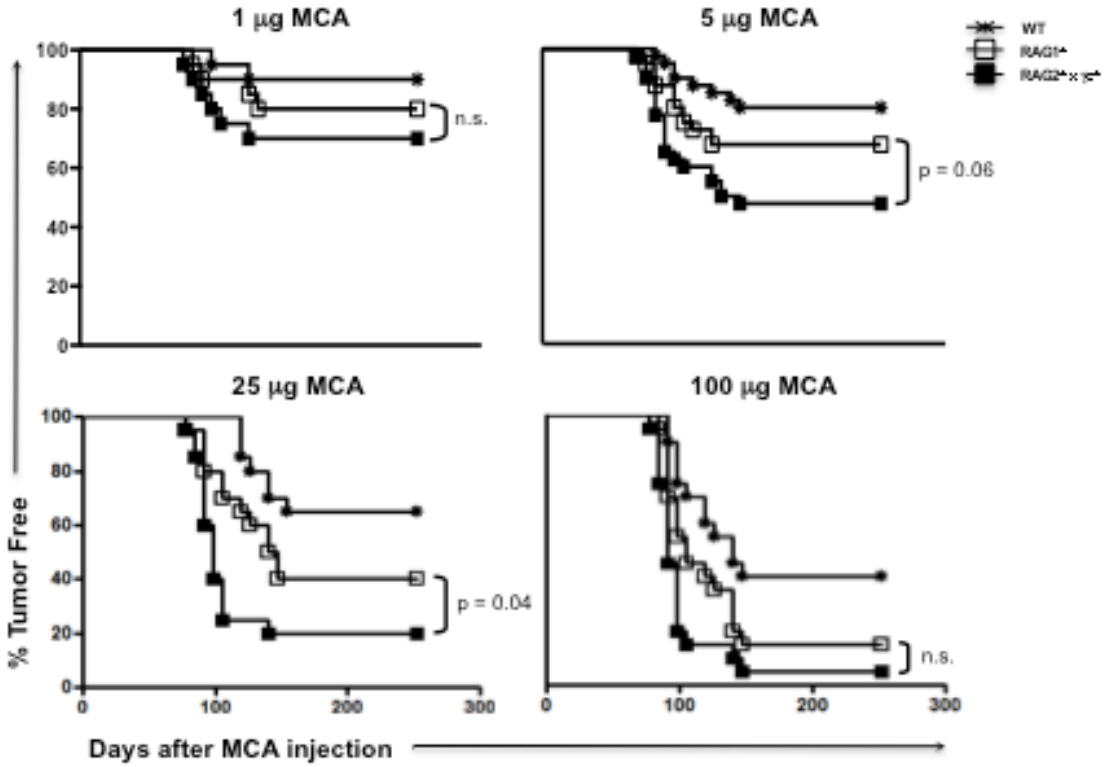

Figure 1.1 RAG2$^{-/-}$x γc$^{-/-}$ mice are more susceptible to MCA-induced sarcomas than syngeneic RAG2$^{-/-}$ and WT mice. The indicated dose of MCA was injected into the subcutaneous space of mice, and sarcoma formation was monitored over time. All cohorts consisted of 20 mice. Tumor positive mice were defined as those that harbored a progressively growing mass $\geq$ 25 mm^2. Similar results were found in a repeat experiment that included the 5 and 25 mg doses.

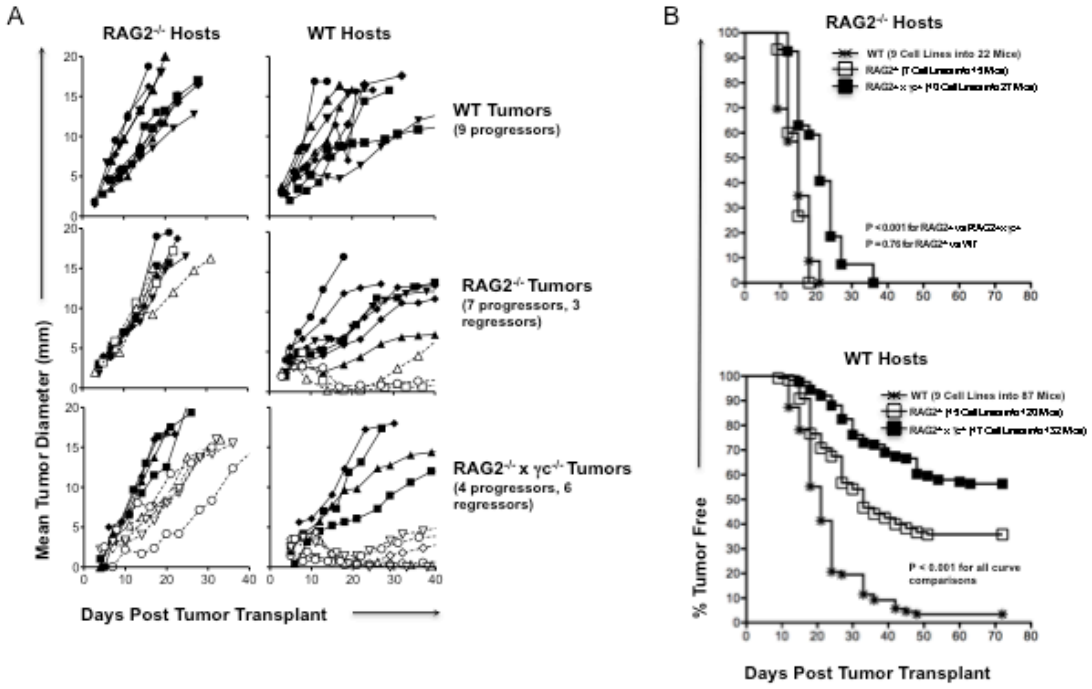

Figure 1.2 A majority of MCA-induced sarcoma cell lines derived from RAG2$^{-/-}$ x γc$^{-/-}$ mice cannot form tumors when transplanted into syngeneic WT mice. MCA-induced sarcoma cell lines were derived from tumors generated in syngeneic C57BL/6-strain WT, RAG2$^{-/-}$, and RAG2$^{-/-}$ x γc$^{-/-}$ mice. These cell lines were transplanted into syngeneic RAG2$^{-/-}$ ($n \geq 2$ for each cell line) or WT ($n \geq 5$ for each cell line) hosts, and tumor growth was measured over time. (A) The average growth for each cell line is shown (open symbols = regressor cell lines; closed symbols = progressor cell lines). (B) The percentage of WT mice that developed tumors is shown for group of cell lines. Tumor free mice were defined to have a non-enlarging mass < 9 mm in average diameter. The number of cell lines and mice are indicated in the figure.

Table 1.1 A summary of 2 independent MCA induction immunoediting experiments. A total of 71 MCA sarcoma cell lines were generated from the indicated mice and then transplanted into 474 WT, $RAG^{-/-}$, or $RAG2^{-/-}$x $gc^{-/-}$ mice, and tumor growth was monitored. Regressor frequencies from these experiments (1 & 2) are shown in Figure 1.3.

Tumor group	Growth in WT	Growth in $RAG^{-/-}$	Growth in $RAG^{-/-}xgc^{-/-}$
9 WT tumors into 87 WT or 22 RAG hosts (exp 1)	**97% (84/87)**	**100% (22/22)**	**N.D.**
15 RAG tumors into 120 WT or 7 into 15 RAG hosts (exp 1)	**64% (77/120)**	**100% (15/15)**	**N.D.**
17 RAGxgc tumors into 132 WT or 10 into 27 RAG hosts (exp 1)	**46% (61/132)**	**100% (27/27)**	**N.D.**
10 WT tumors into 35 WT or 21 RAGxgc hosts(exp 2)	**100% (35/35)**	**N.D.**	**100% (21/21)**
10 RAG tumors into 50 WT or 30 RAG hosts (exp 2)	**60% (30/50)**	**100% (30/30)**	**N.D.**
10 RAGxgc tumors into 50 WT or 30 RAGxgc hosts (exp 2)	**30% (15/50)**	**N.D.**	**100% (30/30)**

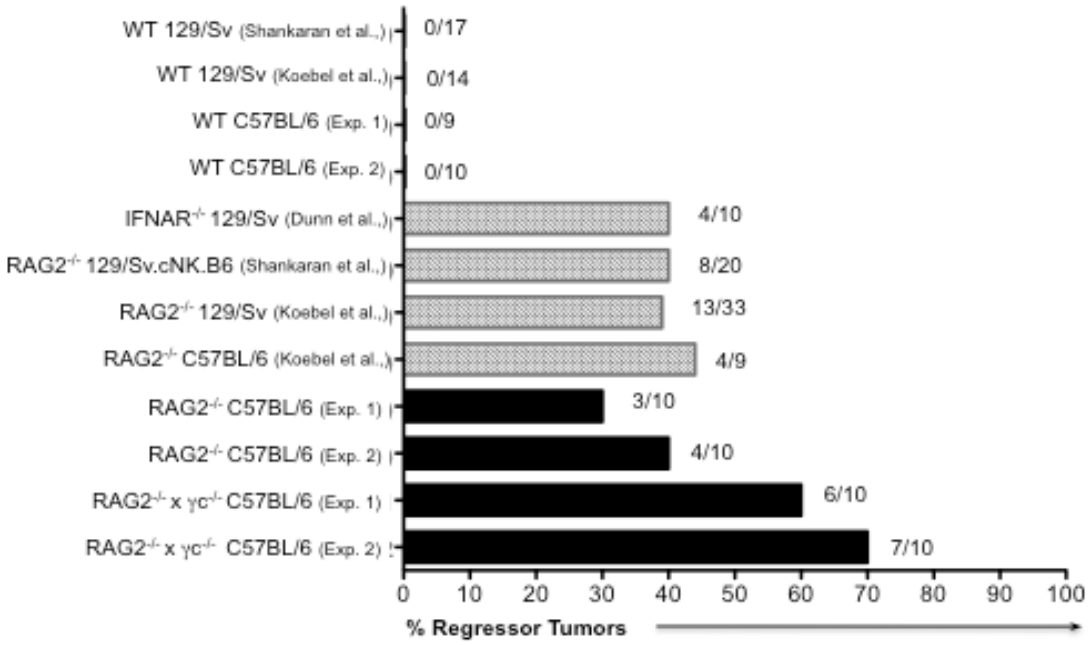

Figure 1.3 The frequency of regressor cell lines is greater from tumors generated in RAG2$^{-/-}$ x γc$^{-/-}$ mice compared to WT and other immune deficient mice. A summary of two MCA-induction experiments performed in this manuscript is plotted in the context of previous MCA-induction experiments. Previously published experiments are included for comparison purposes and are from references[18,22,39]. Absolute numbers of regressors/total number of cell lines tested is shown next to the bar for each experiment.

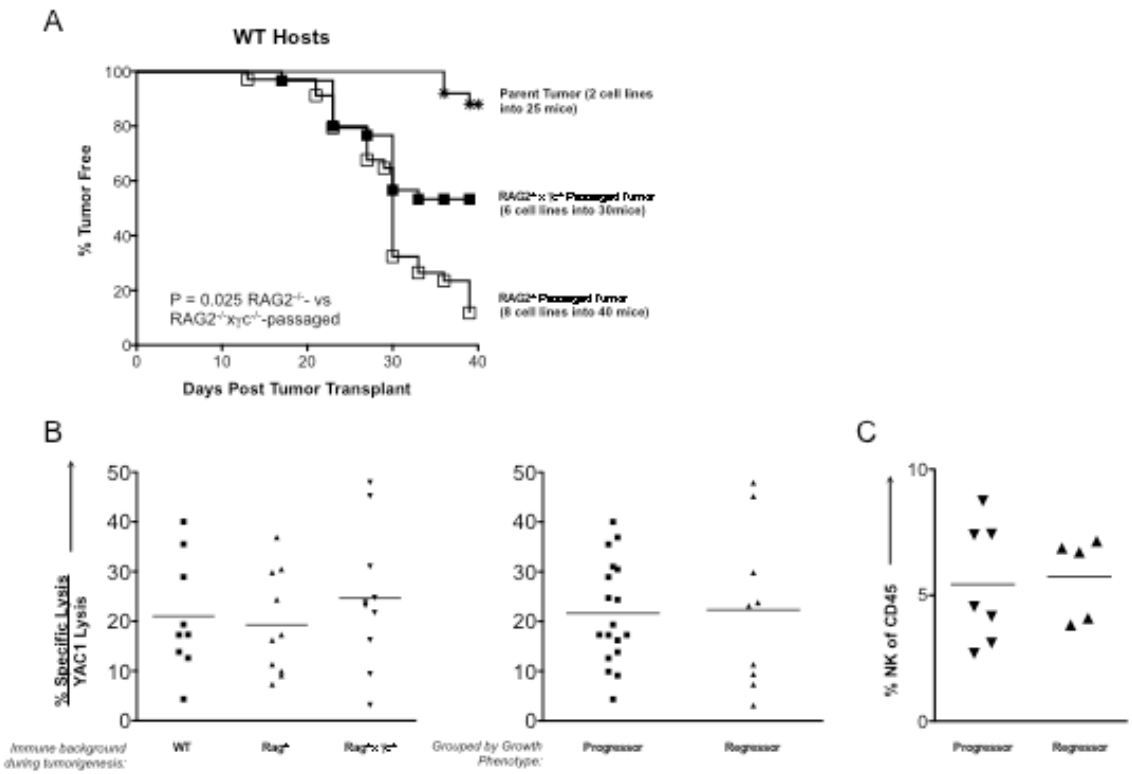

Figure 1.4 RAG2$^{-/-}$ x γc$^{-/-}$ regressors are edited when transplanted into RAG2$^{-/-}$ mice, but are not specifically recognized by NK cells. Two independent MCA-induced sarcoma cell lines generated from RAG2$^{-/-}$ x γc$^{-/-}$ mice were transplanted into syngeneic RAG2$^{-/-}$ x γc$^{-/-}$ or RAG2$^{-/-}$ mice, and tumor masses were harvested at day 25 and converted into "passaged" daughter cell lines, which were transplanted into syngeneic WT mice (number of cell lines and mice are shown in the figure), and (A) the percentage of WT mice that remained tumor free is shown for each group of cell lines. Tumor free mice were defined to have a non-enlarging mass < 9 mm in average diameter by day 40. (B) MCA sarcoma cell lines were cultured with IL-2 activated NK cells in a 5-hour chromium release cytotoxicity assay and specific lysis normalized to YAC-1 specific lysis is plotted for each cell line based on (A) immune background and phenotype. (C) Regressor and progressor cell lines were transplanted into RAG-deficient mice and analyzed for NK cells.

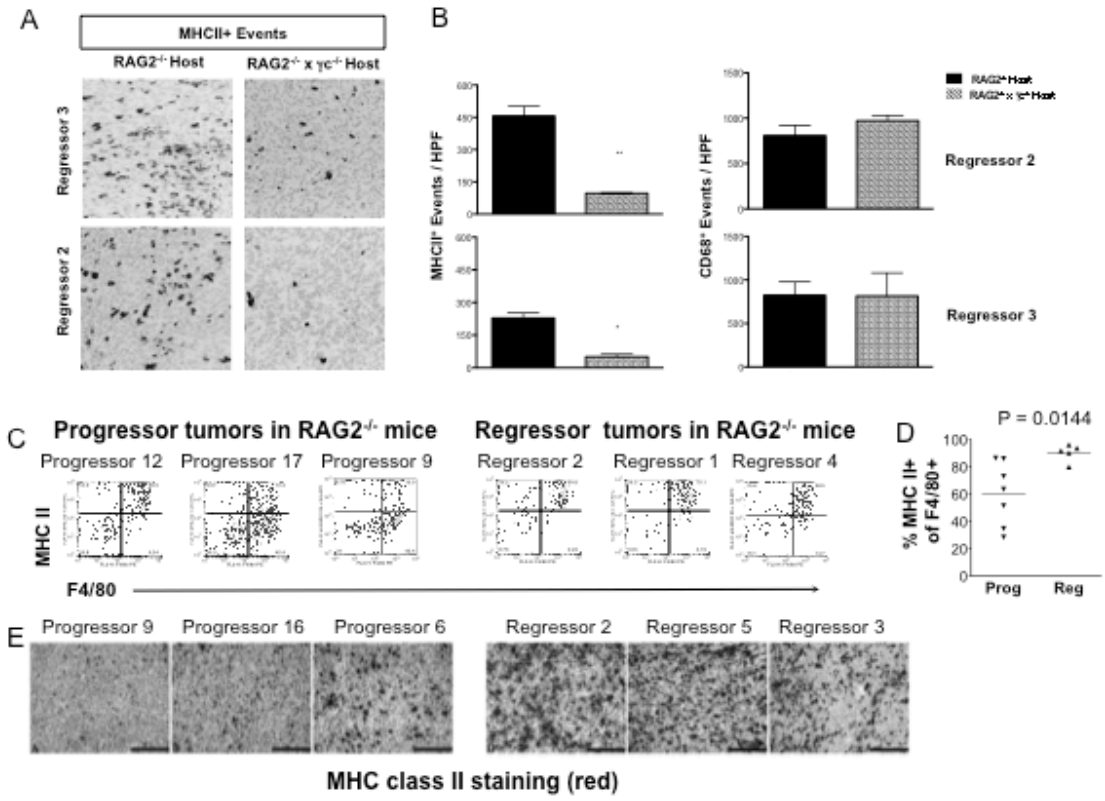

Figure 1.5 MHC class II macrophages preferentially infiltrate in unedited regressors. (A) Representative images of tumor sections from RAG2$^{-/-}$ or RAG2$^{-/-}$ x γc$^{-/-}$ hosts stained for MHC class II. (B) Quantification of MHC class II+ events and CD68+ events in tumor sections is shown. (HPF = high power field at 200x magnification). Regressor and progressor cell lines were transplanted into RAG2-deficient mice and analyzed for (C, D, E) activated MHC class II+ macrophages. (C) Representative FACS plots of 3 regressor and 3 progressor tumors are shown. Cells were gated on a CD45^{+}PI^{-} population. (D) Percentages of activated monocyte-lineage (F4/80^{+}) cell populations are shown for regressor and progressor tumor masses. Each symbol represents a different tumor cell line transplanted into 1-3 RAG2$^{-/-}$ mice. (E) Frozen tumor cross sections of progressor and regressor tumor masses growing in RAG2$^{-/-}$ mice were stained with anti-I-A/I-E (MHC class II). Nuclei were counterstained with hematoxylin. Scale bar = 100 microns. **$p < 0.01$. Error bars are represented by $\pm$ SEM. IHC results were reproduced at least once.

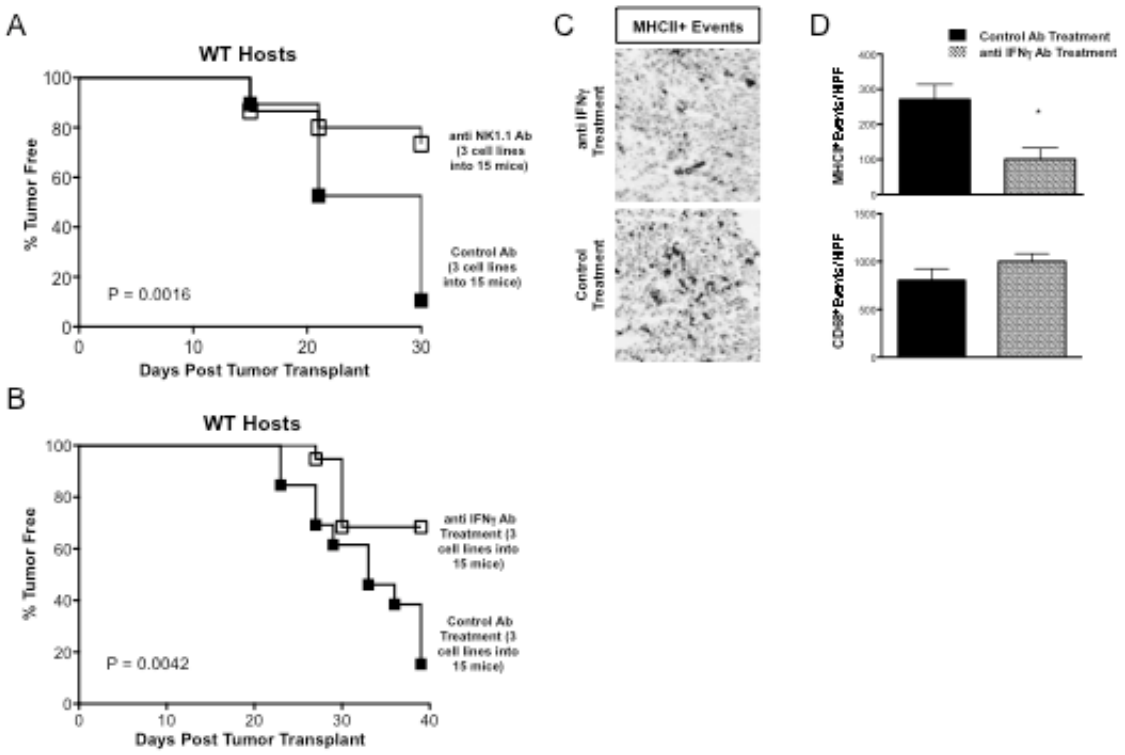

Figure 1.6 NK cells and IFN-g are necessary for innate editing of a regressor tumor and M1 macrophage accumulation. Regressor cell line 2 was transplanted into $RAG2^{-/-}$ mice treated with anti-NK1.1, IFN-g blocking antibody or control antibody, tumor growth was measured, and passaged cell lines were generated. (A,B) The passaged cell lines were then transplanted into syngeneic WT hosts (number of cell lines and mice are indicated in the figure) and tumor free survival was measured. Tumor free mice were defined to have a non-enlarging mass < 9 mm in average diameter by day 40. (C) Tumor sections from $RAG2^{-/-}$ hosts were stained for MHC class II and (D) quantitated. (HPF = high power field at 200x magnification). *$p < 0.05$. Error bars are represented by $\pm$ SEM. Results were reproduced at least once.

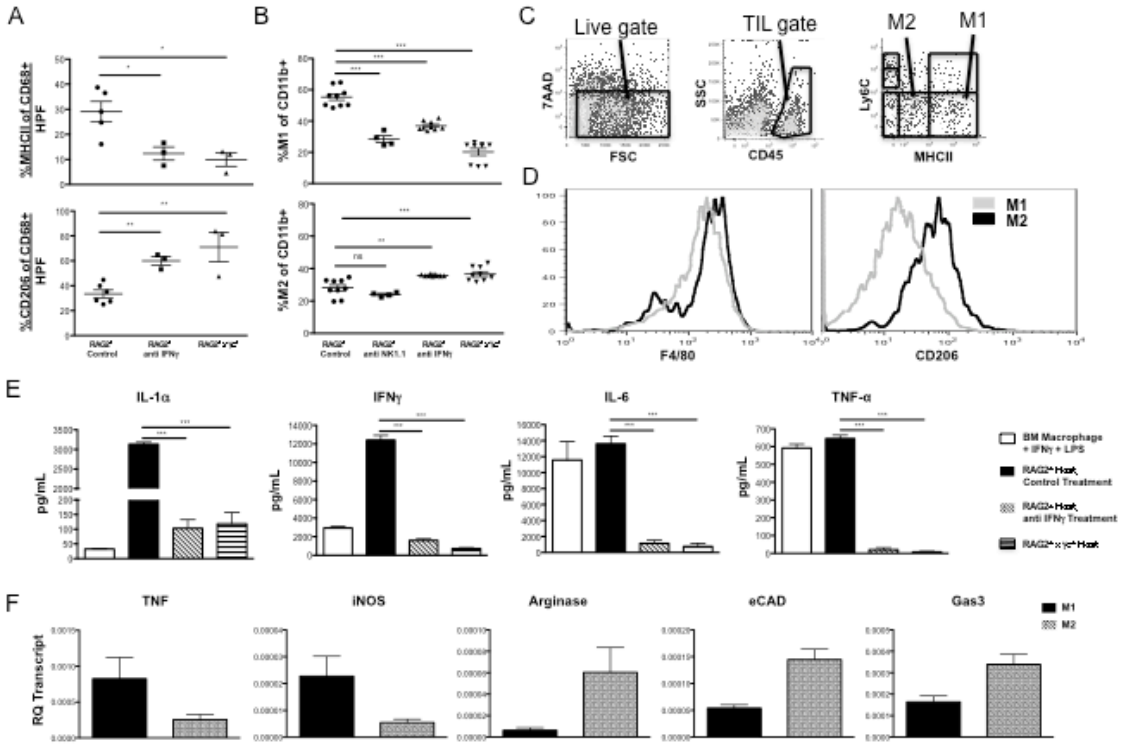

Figure 1.7 NK cells and IFNy are required to polarize tumor associated macrophages towards an M1-type phenotype. Regressor cell line 2 was transplanted into syngeneic $RAG2^{-/-}$ mice (injected with either isotype control, anti-NK1.1, or anti-IFNg monoclonal antibodies) or $RAG2^{-/-}$x $gc^{-/-}$ mice. Tumor masses were harvested 15 days after transplantation, disaggregated into single cell suspensions, and (A) analyzed by immunohistochemistry or (B, C) flow cytometry to measure the percentage of M1 and M2 macrophages as defined by MHC class II and CD206 expression of $CD68^{+}$ events per HPF (for IHC) or MHC class II and Ly6C expression in $CD11b^{+}$ populations (for FACS), respectively. (C, D) An example of the flow cytometry gating to quantitate M1 and M2 macrophages. M1 macrophages are 7AAD-, CD45+, Ly $6C^{lo}$, MHC class II^{hi}, F4/80+, $CD206^{lo}$ cells. M2 macrophages are 7AAD-, CD45+, $Ly6C^{lo}$, MHC $classII^{lo}$, F4/80+, $CD206^{hi}$ cells. (E) Cultured supernatant from single cell suspensions were assessed for production of the indicated cytokines after 24 hours of culture. (HPF = high power field at 200x magnification). *$p < 0.05$, **$p < 0.01$, ***$p < 0.001$. Error bars are represented by $\pm$ SEM. Each symbol represents a different mouse. Results were reproduced at least once.

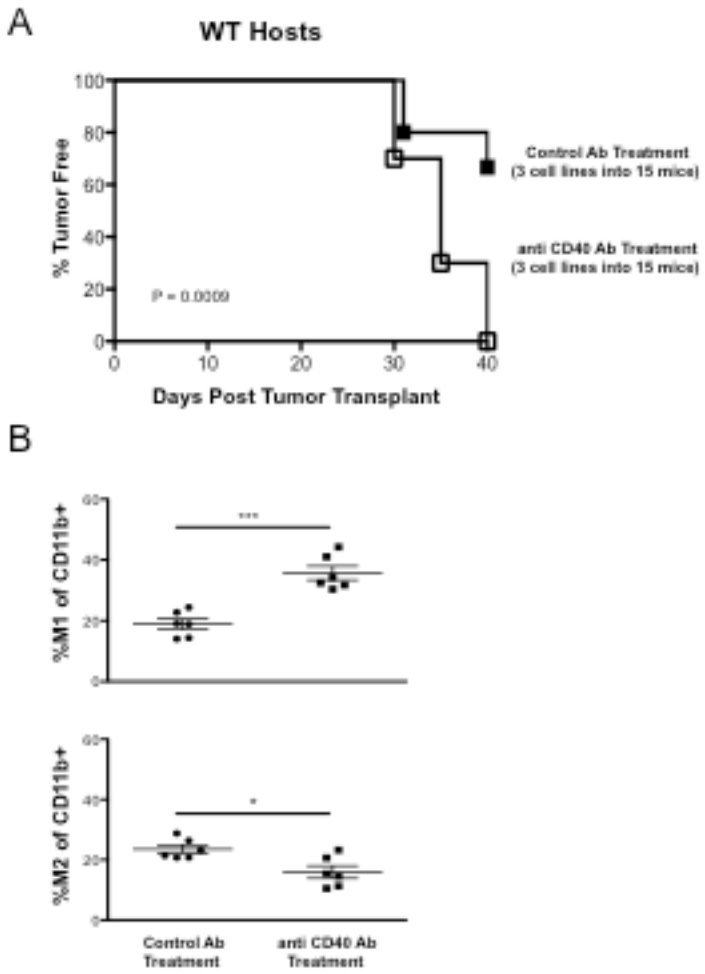

Figure 1.8 In vivo administration of CD40 agonist in RAG2$^{-/-}$x γc$^{-/-}$ mice induces effective immunoediting and intratumoral M1 macrophages. Regressor cell line 2 was transplanted into RAG2$^{-/-}$x γc$^{-/-}$ mice receiving a single dose of either control rat IgG or anti-CD40 agonistic monoclonal antibodies on day 5. Tumor growth was measured over time. (A) Tumor masses were converted into passaged daughter cell lines which were transplanted into syngeneic WT mice and assessed for tumor formation (number of cell lines and mice are indicated in the figure). Tumor free mice were defined to have a non-enlarging mass < 9 mm in average diameter by day 40. (B) At day 15 after transplantation, tumor masses were disaggregated into single cell suspensions and the percentage of M1 (top panel) and M2 (bottom panel) macrophages were quantified in CD11b^{+} events for each condition. *$p < 0.05$, ***$p < 0.001$. Error bars are represented by $\pm$ SEM. Each symbol represents a different mouse. Results were reproduced at least once.

CHAPTER 2: TUMOR-EXPRESSED IL-17D RECRUITS NK CELLS TO REJECT TUMORS

We hypothesized that tumor-expressed factors in unedited tumors can activate host tumor immunosurveillance and that these factors must be silenced in order for tumors to survive in immune competent individuals. A microarray analysis comparing immunogenic, regressor tumors to non-immunogenic, progressor tumors identified the cytokine IL-17D as one expressed and secreted to a higher extent in regressor tumor cells. IL- 17D overexpression in various progressor tumor cell lines was sufficient to mediate tumor rejection or regression in syngëneic WT recipients. Importantly, we determined that IL-17D overexpression does not impact tumor cell growth rate in vitro or tumor development upon transplantation in immunodeficient mice, suggesting that the primary role for tumor-expressed IL-17D is to initiate antitumor immunity. Accordingly, we found that NK cells are present at higher percentages within progressor tumors expressing IL-17D as compared to controls, and that M1 tumor-associated macrophages (TAM) preferentially accumulate in the presence of recruited tumor-infiltrating NK cells. We found that IL-17D is not responsible for directly recruiting NK cells and M1 TAMs, but, rather, functions to stimulate tumor endothelial cells to produce MCP-1 that in turn, recruits NK cells into the tumor microenvironment and, subsequently polarizes TAMs toward an M1. We then tested whether MCP-1 production and resultant NK cell recruitment was required for IL-17D mediated antitumor immunity by depleting MCP-1 or NK cells in WT mice transplanted with IL-17D overexpressing progressor tumor cells. Over- expression of IL-17D in progressors failed to inhibit tumor growth upon blockade of either NK cells or

MCP-1, demonstrating that NK cells and MCP-1 are essential for the antitumor effect of IL-17D.

IL-17D Is Highly Expressed by Certain Regressor, but Not Progressor, Tumors

To identify regressor-expressed molecules that could mediate rejection of progressor:regressor mixtures, we performed microarray studies of 8 independent regressor and 16 independent progressor tumor cell lines (Fig. 2.1). We found that the novel cytokine IL-17D was highly upregulated in regressors compared to progressors as shown by intracellular flow cytometry (Fig. 3.1 A-B) and qRT-PCR (Fig. 3.1 C). These results suggest that IL-17D was secreted in vitro at higher levels by regressor versus progressor tumor cell lines.

IL-17D Promotes Progressor Tumor Rejection but Is Not Required for Regressor Tumor Rejection

We then explored whether IL-17D expression in progressor tumors could mediate their rejection in WT mice in the absence of other regressor-associated molecules (Fig 2.2). In four of the six progressor cell lines tested, the overexpression of IL-17D led to complete rejection (F244 and d30m1; Fig 2.2 A top) or a significant delay in growth (B16.OVA and LLC; Fig 2.2 A bottom) in WT mice. This effect of IL-17D was due to adaptive immune cells, because in vitro (not shown) and in vivo growth kinetics in *rag2*$^{-/-}$

mice remained unchanged (Fig 2.2 B). To demonstrate the antitumor efficacy of IL-17D on pre-established tumors, we generated a progressor tumor cell line (F244TR17D) that expressed IL-17D upon administration of doxycycline. Induced expression of IL-17D led to tumor rejection (Fig 2.2 C).

IL-17D Expression Enhances Recruitment of NK Cells in Progressor and Regressor Tumors

To define the mechanism of IL-17D-mediated tumor rejection, we characterized tumor-infiltrating immune cells in tumors with high and low levels of IL-17D. We found an approximately 2-fold increase in the amount of NK cells in tumors with high versus low IL-17D (Fig 2.3 A-B). These NK cells had similar phenotype to splenic NK cells and did not display markers found in immunoablative NK cells[60] or interferon-producing killer dendritic cells. Notably, NK cells were required for tumor rejection, because mice treated with anti-NK1.1, but not control immunoglobulin G (IgG), failed to reject the IL-17D-overexpressing tumors (d30m1, F244) (Fig 2.3 C). The recruitment of NK cells likely mediates IL-17D's antitumor activity, as we did not observe enhanced numbers of either neutrophils or monocytes in tumors expressing high versus low levels of IL-17D and neutrophils were not required for IL-17D-mediated tumor rejection (data not shown).

Because it is known that NK-dependent tumor rejection can lead to priming of adaptive immune responses[25,61] we then tested whether mice that had rejected IL-17D-overexpressing tumors could reject a rechallenge with untransduced progressor tumors.

Indeed, we found that parental cells were rejected in primed mice (Fig 2.3 C), confirming that edited tumors possess antigens and that initiating the ‘‘correct’’ innate cell response (via IL-17D) can result in productive antigen-specific antitumor responses.

Previously, we have found a requirement for NK cells and interferon γ (IFNγ) in the accumulation of M1 macrophages in regressor tumors during cancer immunoediting[62]. We also observed an approximately 1.5-fold enhancement in the accumulation of M1 macrophages in progressor tumors overexpressing IL-17D (Fig 2.3 D), whereas silencing of IL-17D in regressor tumors reduced M1 macrophages by approximately 2-fold in both WT and *rag2*$^{-/-}$, but not *rag2*$^{-/-}$ x *γc*$^{-/-}$, hosts, which are deficient in NK cells (Fig 2.3 D).

IL-17D Recruits Innate Immune Cells in an Air Pouch Model of Inflammation

To show directly whether IL-17D can induce the recruitment of immune cells, we used an in vivo air pouch model of inflammation in WT mice. Sterile air pouches become well vascularized after a period of 7 days (data not shown) and recruit immune cells rapidly after administration of lipopolysaccharide (LPS). Indeed, we found that LPS, IL-17A, and IL-17D significantly recruited CD45+ immune cells into air pouches compared to PBS control (Fig 2.4 A). When we examined the composition of the immune cells, we found that LPS and IL- 17A recruited more neutrophils than any other cell type, whereas neutrophils constituted a smaller percentage of cells recruited by IL-17D (Fig 2.4 B). Interestingly, IL-17D recruited significantly more NK cells (Fig 2.4 C), but not monocytes (Fig 2.4 C), neutrophils, or macrophages, compared to LPS and IL-17A. We found that the

IL-17D-recruited NK cells were mostly CD27high, which could be a semimature population of NK cells that may participate in IFNγ-dependent T cell priming in lymph nodes (Fig 2.4 D). Interestingly, IL-17D recruited approximately twice the amount of $CD27^{high}CD11b^{low}$ NK cells as LPS, with no significant recruitment of mature $CD27^{low}$ NK cells (Fig 2.4 D).

IL-17D Indirectly Recruits NK Cells In Vivo by Stimulating the Production of MCP1

Because IL-17A is known to induce IL-8 from endothelial cells to recruit neutrophils, we examined whether IL-17D utilized a similar mechanism. Indeed, we found that IL- 17D induced the expression of MCP-1 in mouse air pouch lavage fluid (Fig 2.5 A). We then repeated air pouch experiments in the presence of blocking antibodies specific for MCP-1 and found that anti-MCP1, but not control IgG, completely inhibited IL- 17D-mediated recruitment of NK cells (Fig 2.5 B). Furthermore, qRT-PCR analysis of purified tumor endothelial cells from two IL-17D-overexpressing tumors showed a 4–17 times increase in MCP-1 transcript compared to control tumors, respectively (Fig 2.5 C). Notably, depletion of MCP-1 led to increased growth of two IL-17D-over-expressing tumors (Fig 2.5 D).

DISCUSSION

The IL-17 family of cytokines promotes immune responses by inducing the expression of pro-inflammatory cytokines and chemokines, leading to recruitment of neutrophils, and other innate immune cells[63]. IL-17A/IL-17F are produced by Th-17 cells and are involved in autoimmune disease and host responses to tissue infection. IL-17C may have similar inflammatory functions to IL-17A/IL-17F, although IL-17C is expressed in epithelial cells and is induced by microbial ligands. Our discovery that IL-17D is expressed outside the immune system and functions to recruit NK cells suggests that the IL-17 family may have evolved to evoke distinct arms of the immune response, presumably to deal with specific pathogen insults. We speculate that similar to IL-17C, the expression of IL-17D in non-immune tissues may mediate local anti-viral immunity through the recruitment of NK cells. Notably, our preliminary studies indeed have found increased IL-17D transcripts in virus-infected skin (RSK and JDB, preliminary observations). Future studies on the endogenous role of IL-17D (in the context of infection, autoimmunity, and cancer) and its regulation are certainly warranted.

Our studies have shown that IL-17D is poorly expressed in cancer cells that grow progressively (mouse MCA-induced sarcomas and certain human cancers) but, comparatively, can be highly expressed in certain immunogenic MCA-induced sarcoma cells and in normal human tissue. It is not clear what regulates the constitutive expression of IL-17D in certain cells. Since normal human tissue is not infiltrated with NK cells, it is possible that the detection of IL-17D in normal tissues is not correlated with its secretion. We speculate that the constitutive presence (but not secretion) of IL-17D in certain normal cells could be to function as a danger signal and mediate sterile inflammation, similar to

IL-1 and HMGB1[64]. Nevertheless, it is clear that high expression of IL-17D is not compatible with tumor progression, since advanced stage human and edited mouse cancer cells have low levels of IL-17D, and the ectopic expression of IL-17D in progressor cells leads to NK-dependent tumor rejection. Although overexpression of immune cell-derived chemokines and cytokines such as GM-CSF and IL-15 have already been demonstrated to have potent antitumor efficacy[65], our study elucidates a tumor-derived cytokine expressed by highly immunogenic tumors that can mediate the rejection of poorly immunogenic tumors.

It should be noted that not all regressors have high levels of IL-17D and that there are multiple genes that are differentially expressed in regressor, thus indicating that IL-17D is one of many genes that could participate in tumor surveillance. This is likely due to the heterogeneity and redundancy that is inherent in our system (and possibly in normal tumor surveillance mechanisms). For example, we have found that some regressors are well recognized by NK cells whereas others are not, and this is not always correlated with NKG2D ligand expression[38] even though NK cells and NKG2D are important for tumor surveillance[23,49]. Furthermore, some regressors require type I IFN for their rejection whereas others do not[22], even though IFNAR$^{-/-}$ mice lacking IFNa/b responsiveness are more susceptible to cancer[10,22], and IFNa/b is used in the treatment of melanoma. Similarly, we have found that silencing of IL-17D in regressors leads to growth delay, but the cells are still rejected (data not shown). We speculate that certain highly antigenic regressors may not require IL-17D for their rejection, whereas the rejection of poorly immunogenic progressors could be facilitated by IL-17D-dependent recruitment of NK cells, thereby providing an optimized microenvironment for priming adaptive immunity,

as shown for DC-mediated priming of T cells in the lymph node. We therefore conclude that IL-17D is one of many genes that regressor cells produce that can stimulate antitumor immunity. The identification of other genes that can differentiate regressor from progressor cell lines will involve future studies likely combining proteomic, gene expression, and exome sequencing approaches[66].

We have shown that IL-17D can be induced to reject small, established tumors, but cannot reject larger or more aggressive cancers. It is now accepted that established tumors are embedded in a microenvironment with immune suppressive cells including myeloid-derived suppressor cells and Tregs and factors such as PD-L1 and IDO (Muller and Scherle, 2006; Zou, 2005). Some of these factors, such as Tregs, have been shown to inhibit NK-mediated tumor surveillance (Smyth et al., 2006). Notably, the immune suppressive environment can be targeted by treatment with anti-CTLA4 (Curran et al., 2010; van Elsas et al., 2001) and/or anti-PD-1 (Hirano et al., 2005). These results suggest that the antitumor efficacy of recombinant IL-17D on pre-established tumors could be enhanced with combination therapy. Future studies will address the potential synergy between IL-17 and other immune therapies, including NK cell activators and checkpoint blockade, thereby boosting both the innate and adaptive arms of antitumor immunity to provide long-lasting tumor remission.

Chapter 2, in full, is an adapted version of the material as it appears in Cell Reports, 2014, Timothy O'Sullivan, William Vermi, Catherine M Koebel, Cora Arthur, J Michael White, Ravi Uppaluri, Daniel M Andrews, Shin Foong Ngiow, Michele W L Teng, Mark J Smyth, Robert D Schreiber, and Jack D Bui; Elsevier Ltd. The dissertation author was the second author of this paper.

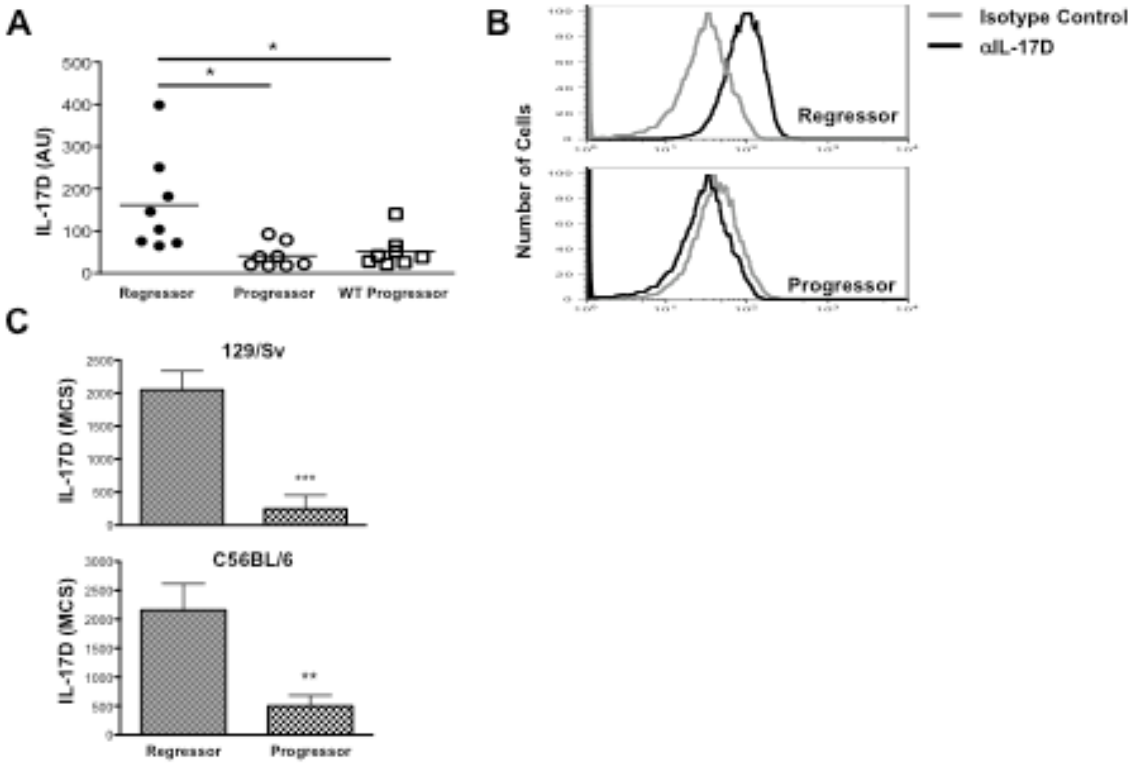

Figure 2.1 IL-17D is highly expressed in some regressor cell lines and is downregulated in progressor tumor cell lines and severa human cancer samples. (A) Plotted microarray data of *IL-17D* gene expression of regressor (n = 8) and progressor (n = 16) tumor cell lines. (B) qRT-PCR analysis of independent regressor (n = 4) and progressor (n = 4) tumor cell lines. (C) Quantitated IL-17D intracellular protein expression of 129/Sv *RAG2*$^{-/-}$-derived regressor (n = 3) and progressor (n = 3) tumor cell lines incubated with or without brefeldin A and monensin. IL-17D mean channel shift (MCS) values are calculated by taking the mean florescence of IL-17D intracellular protein signal and subtracting the mean fluorescence signal of the isotype control stain for the same tumor cell line sample. Data are representative of two independent experiments. (*P < 0.05, **P < 0.01

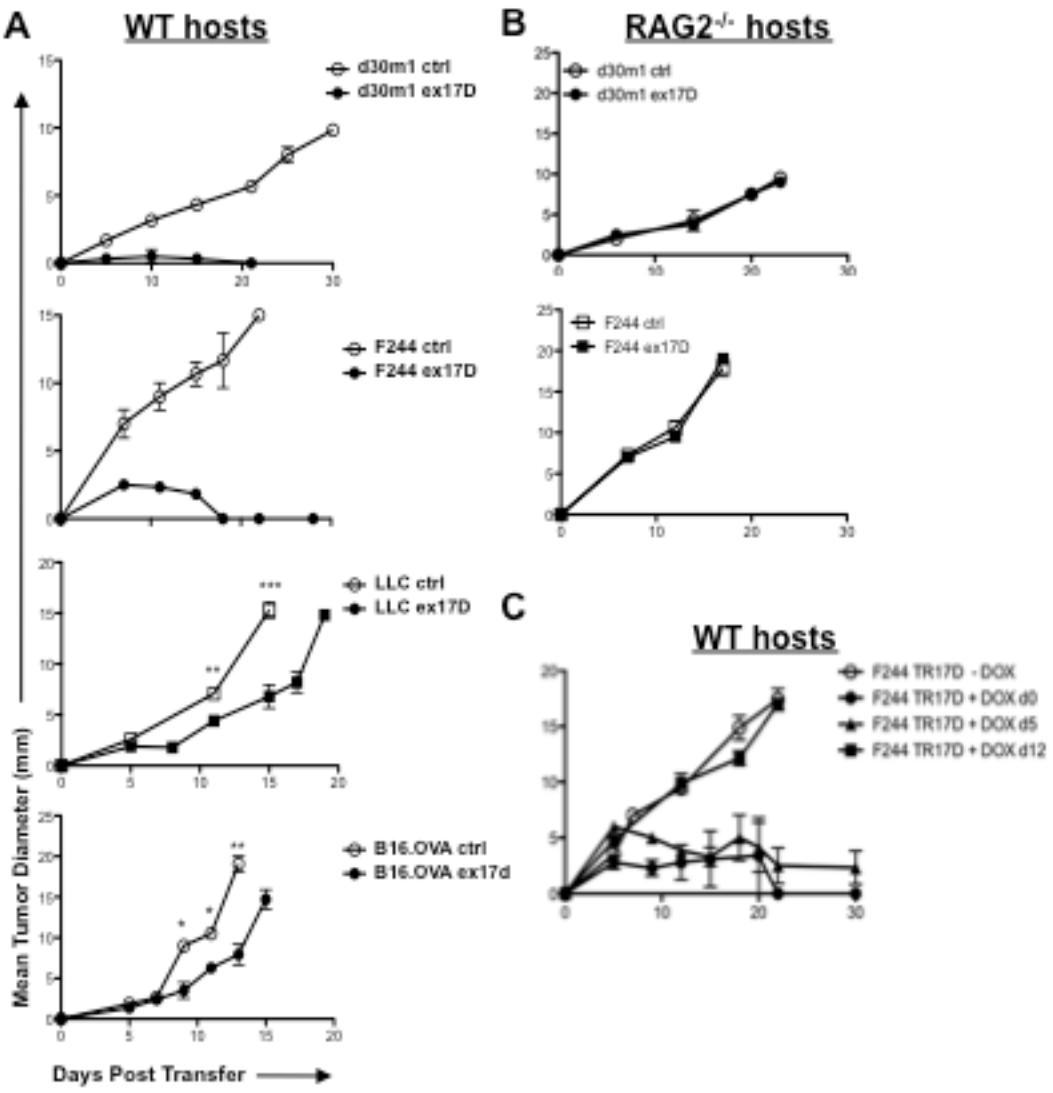

Figure 2.2 Expression of IL-17D mediates progressor tumor rejection. A) Tumor growth of indicated (ctrl, sh17D) regressor tumors transplanted into WT mice (n = 5 for each tumor cell line). (B) Tumor growth of indicated (ctrl, ex17D) progressor tumors transplanted into WT mice (n = 5 for each tumor cell line). (C) Tumor growth of inducible IL-17D progressor tumor cell line transplanted into WT mice receiving water or doxycycline continuously from day 0 (n = 5), day 5 (n = 5), or day 12 (n = 5). Samples were compared using an unpaired, two-tailed Student's t test with Welch's correction. Error bars are depicted as ±SEM (*$p < 0.05$, **$p < 0.01$, ***$p < 0.001$).

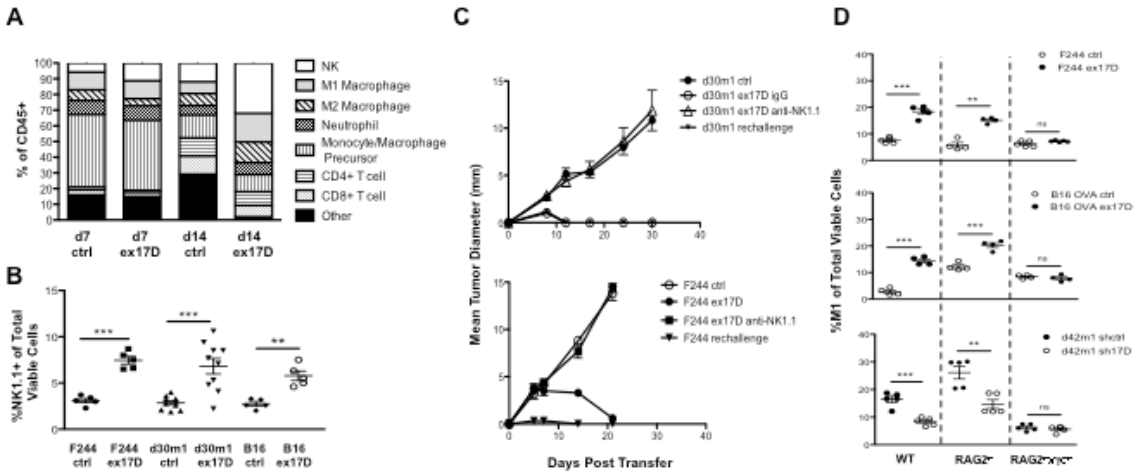

Figure 2.3 Overexpression of IL-17D in progressor tumors recruits NK cells that are required for tumor rejection in WT mice and promote M1 macrophage infiltration. (A) Percentage of (7AAD-CD45+, CD3-, NK1.1+) NK cells, (7AAD-, CD45+, CD11b+, Ly6G+, MHCIIlo) neutrophils, (7AAD-, CD45+, CD11b+, Ly6Chi) monocytes/ macrophage precursors, (7AAD-, CD45+, F4/80+, Ly6Clo, MHCIIhi, CD206lo) M1 macrophages, (7AAD-, CD45+, F4/80+, Ly6Clo, MHCIIlo, CD206hi) M2 macrophages, (7AAD-, CD45+, CD3+, CD4+, CD8-) CD4+ T cells, and (7AAD-, CD45+, CD3+, CD4-, CD8+) CD8+ T cell-infiltrating immune cells in F244 ctrl or ex17D tumors on days 7 and 14 posttransplantation in WT mice. (‘‘Other’’ indicates infiltrating Ly6C-MHCII-NK1.1-CD3- immune cells). (B) Percent infiltrating NK cells of total viable (7AAD-) cells from transduced regressor and progressor tumors on day 7 posttumor transplant in WT mice. (C) Tumor growth of IL-17D overexpressing (ex17D) progressor tumors transplanted into WT mice receiving either intraperitoneal injections of anti-NK1.1/control IgG or preimmunized with transplantation of IL-17D overexpressing (ex17D) tumor cell lines. (D) Percentage of M1 macrophages of total viable cells on day 14 posttumor transplant of progressor tumor cell lines into WT, *RAG2*$^{-/-}$, or *RAG2*$^{-/-}$ x $\gamma c^{-/-}$ hosts. Data from (A)–(D) are representative of two independent experiments. Samples were compared using an unpaired, two-tailed Student’s t test with Welch’s correction. Error bars are depicted as ±SEM (**p < 0.01, ***p < 0.001, ****p < 0.0001; NS, not significant).

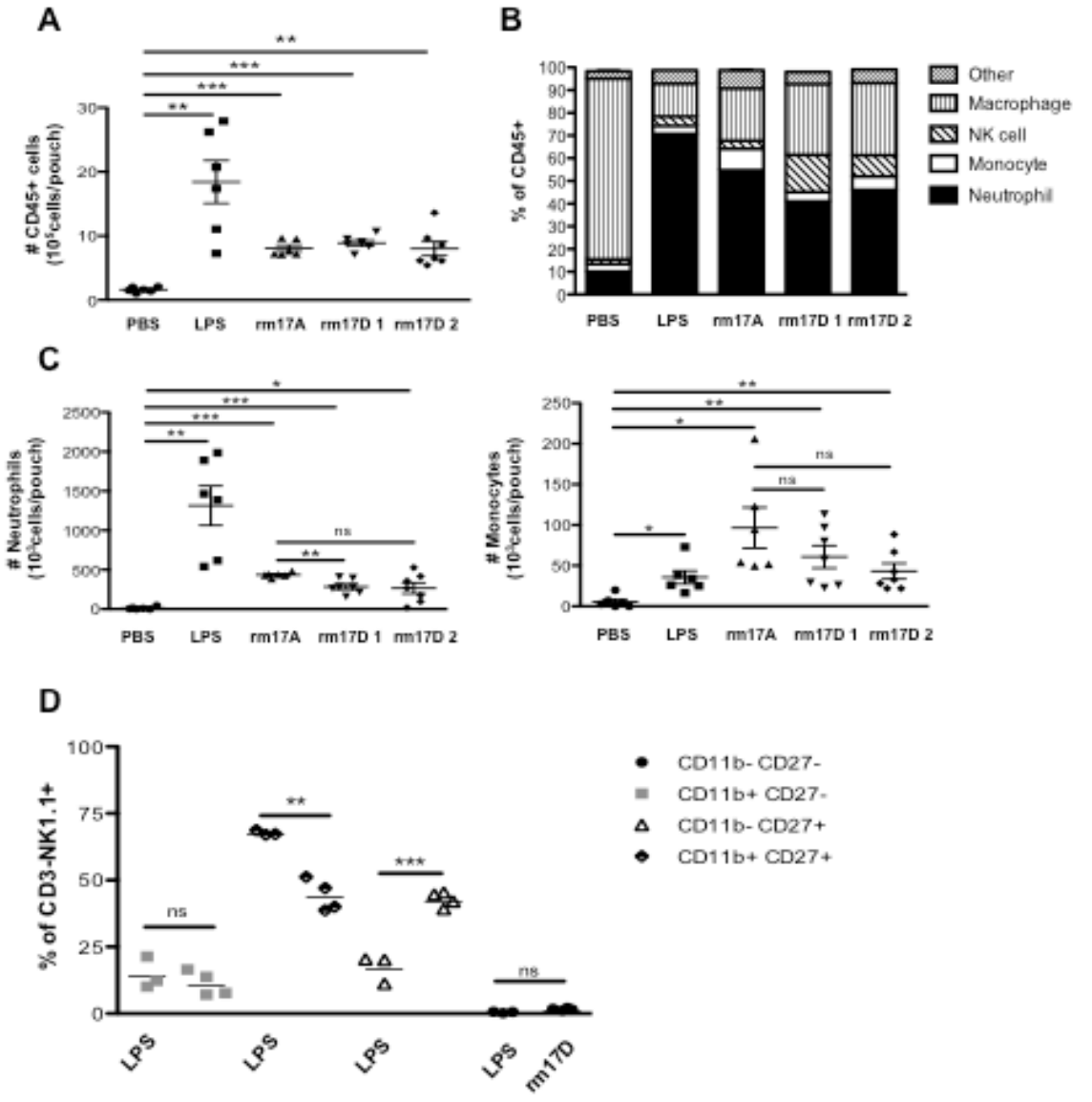

Figure 2.4 Recombinant mouse IL-17D recruits NK cells in an air pouch inflammation model. (A) Total number of infiltrating immune cells per air pouch in WT mice receiving intrapouch injections of PBS, LPS, IL-17A, IL-17D-1 (generated from *E. coli*.), or IL17D-2 (generated from *C. reinhardtii*). (B) Percentages of NK cells, monocytes, neutrophils, and macrophages per air pouch receiving indicated intrapouch injections. (Other indicates CD4+, CD8+ T cells or Ly6C-MHCII-NK1.1-CD3- recruited immune cells). (C) Total number of NK cells and monocytes per air pouch receiving indicated intrapouch injections. (D) Immunophenotypic analysis of infiltrating NK1.1+CD3- NK cells in mouse air pouches receiving intrapouch injections of LPS or rmIL-17D. Data from (A)–(D) are representative of two independent experiments. Each point represents an individual mouse. Samples were compared using an unpaired, two-tailed Student's t test with Welch's correction. Error bars are depicted as ±SEM (*$p < 0.05$, **$p < 0.01$, ***$p < 0.001$).

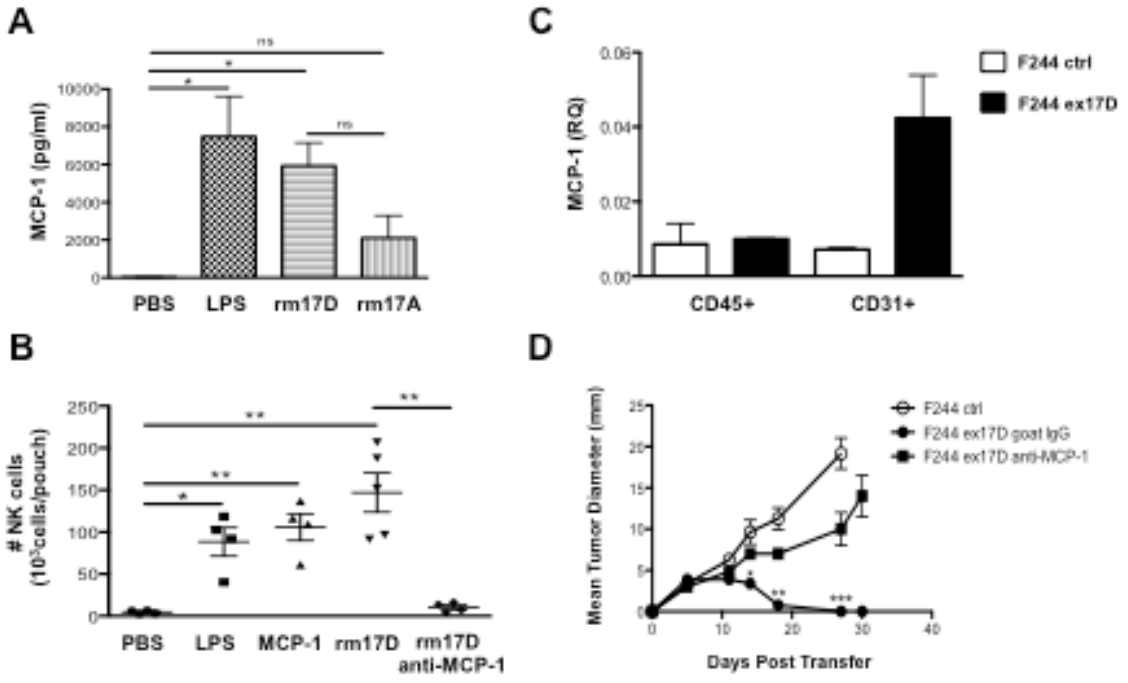

Figure 2.5 IL-17D indirectly recruits NK cells through tumor endothelial cell production of MCP-1. (A) Air pouch lavage fluid chemokine levels of MCP-1. (B) Total number of NK cells per air pouch for WT mice receiving intrapouch injections of PBS, LPS, IL-17A, IL-17D, MCP-1, or IL-17D and anti-MCP-1 monoclonal antibodies. (C) qRT-PCR analysis of MCP-1 expression from purified tumor leukocytes and endothelial cells harvested from day 7 F244 control or ex17D tumors. (D) Tumor growth of F244 control and ex17D tumors transplanted into WT mice receiving either intraperitoneal (i.p.) injections of goat poly-clonal anti-MCP-1 or control goat IgGs. Data are representative of two independent ex- periments. Each point represents a single mouse. Samples were compared using an unpaired, two- tailed Student's t test with Welch's correction. Error bars are depicted as ±SEM (*$p < 0.05$, **$p < 0.01$, ***$p < 0.001$; NS, not significant).

CHAPTER 3: NRF2 INDUCES IL-17D TO MEDIATE IMMUNOSURVEILLANCE

We hypothesized that reactivation of pathology-triggered early stress pathways can activate protective host immunosurveillance. We have direct and compelling evidence that the transcription factor Nrf2 induces the expression of IL-17D by directly binding to the promoter region of the *il17d* gene. Nrf2, recognized as the primary regulator of cellular oxidative stress, is responsible for the induction of genes involved in an array of key cellular programs: primarily - antioxidant defense, oxidant signaling, and drug metabolism; and, secondarily - metabolism, cell proliferation, and proteasome activity[5-8,67,68]. Inappropriate Nrf2 activity contributes to various pathologies, including autoimmunity[69,70], neurodegenerative disorders[71-73], acute lung injury, COPD, chronic kidney disease, diabetes, heart failure, atherosclerosis, IBD, neurodegenerative disorders, sepsis and cancer (see reviews[74-76]). The role of Nrf2 in cancer is complex[77,78]. While Nrf2 protects somatic and premalignant cells from tumorigenesis, it is well documented that Nrf2 can promote the growth and survival of established tumors[79,80]. Nrf2 is a direct downstream target of both intrinsic and extrinsic cellular protective responses, but a direct link has yet to be established between cellular defense via Nrf2 and host defense via immunity. Specifically, it is not known whether cellular stress, leading to the activation of Nrf2, would, consequently, initiate an immune response. We find that Nrf2 regulates IL-17D both in vitro and in vivo during primary tumorigenesis and viral infection; and, we confirm that IL-17D protects the host from primary tumor development as well as viral infection in vivo. Additionally, we show that activation of Nrf2 via topical treatments will induce IL-17D specifically within tumors to initiate

protective antitumor immunosurveillance programs. Our data document a novel link between cellular oxidative stress - resulting from viral infection or tumorigenesis - and the initiation of immunity. We describe an uncharacterized role for the well-studied factor Nrf2 and address the long-standing question of how immune cells are recruited by distressed cells.

Nrf2 induces IL-17D

To explore IL-17D's regulation, we performed a transcription factor binding site (TFBS) analysis of the promoter and intronic regions of the human and mouse *il17d* genes (Fig. 3.1 A). Our analysis revealed several putative binding sites for the transcription factor Nrf2. We characterized putative Nrf2 binding sites as anti-oxidant responsive elements (ARE) [81] (Fig. 3.1 A). Given the abundance of ARE in promoter and intronic regions of *il17d*, we hypothesized that the activation of Nrf2 would induce IL-17D. To test this, we treated murine embryonic fibroblasts (MEFs) and a 3-methylcholanthrene (MCA)-induced sarcoma cell line F244[18,62] with H_20_2, a known potent activator of Nrf2 [82,83] (Fig. 3.1 B). H_20_2 treatments led to significant, dose responsive increases in the transcript of *il17d*. Similarly, activation of Nrf2 with *tert*-butylhydroquinone (tBHQ) resulted in the increase of *il17d* transcript the murine melanoma cell line B16, the human burkitt's lymphoma cell line Ramos and in the MCA-induced sarcoma cell line F244 (Fig. 3.1C).

Next, we determined whether the transcription factor Nrf2 directly binds to the TFBS we identified in our analysis of the *il17d* gene. We performed a ChIP-qPCR in

tBHQ-treated or control-treated B16 cell lines. Cells were fixed and sonicated (not shown) before immunoprecipitation with Nrf2-specific antibody or control IgG. Fractionation and western blot analysis of these B16 cell lines confirmed that Nrf2 preferentially accumulated in the nuclear fractions of treated cells (not shown). qPCR analysis of ChIP fractions revealed two sites upstream of the *il17d* start site where Nrf2 has significant binding following activation (Fig. 3.1 D). These two binding sites for Nrf2 corresponded to Nrf2 target ARE elements identified at 4195, 4860 and 3730 bp upstream of *il17d*'s start site (Fig. 3.1 D). qPCR analysis of the known gene target for Nrf2, HMOX-1, also indicated Nrf2 binding following tBHQ treatment in the B16 cell line.

TFBS analysis with the ENCODE UCSC browser revealed that other transcription factors might bind and regulate IL-17D (data not shown), indicating that Nrf2 may not be wholly responsible for the induction of IL-17D. In order to examine the necessity of Nrf2 for the induction of IL-17D, we activated Nrf2 in the F244 or B16 cell lines in the presence of siRNA specific to Nrf2 (Fig. 3.1 E). Knockdown of Nrf2 in B16 and F244 (~80%) was sufficient to block the induction of IL-17D following activation of Nrf2 with either H_20_2 or tBHQ. Altogether, we found that Nrf2 not only directly bound to the IL-17D promoter region but also was required for efficient induction of IL-17D by oxidative stress.

Nrf2 and IL-17D are expressed in the primary human and mouse tumors and during viral infection

To determine the relevance of Nrf2's regulation of IL-17D in vivo, we examined the expression of IL-17D and Nrf2 in human and mouse tumors and during viral infection in mice. Using human tumor data sourced from The Cancer Genome Atlas (TCGA), we partitioned human melanoma samples into high and low IL-17D expressors and found that IL-17D and Nrf2 expression directly correlated with one another but inversely correlated with KEAP-1 expression (Fig. 3.2 A). We also found similar expression patterns in human liposarcomas. Moreover, we found that a high level of IL-17D expression in human tumors – melanoma and sarcoma - confers a survival advantage (Fig. 3.2 B). An analysis of our MCA-sarcoma tumor cell lines similarly demonstrated that Nrf2 and IL-17D are co-expressed in murine tumor cell lines (Fig. 3.2 C). As shown previously[84,85] we found that MCA-sarcoma cell lines expressing high IL-17D levels are generally regressive in their growth in vivo compared with low IL-17D expressing tumors, paralleling the survival advantage conferred by high IL-17D expression in human tumors [84,86] (Fig. 3.2 D). Together, these data suggest that Nrf2 regulates IL-17D during primary tumor formation in both human and mouse systems in order to initiate productive antitumor immune responses leading to tumor regression and prolonged survival.

IL-17D can recruit NK cells in vivo[84,85,87]. As NK cells are critical for immune-mediated clearance of viral infections[4,8], we speculated that IL-17D may play an important role in antiviral immunity. To examine this, we first measured Nrf2 and IL-17D following infection with viruses known to require NK cells for clearance: Vaccinia Virus (VV)[88] and Murine Cytomegalovirus (MCMV)[89]. Following infection with VV or MCMV in vitro, we observed an increase in the transcript levels of IL-17D in both infected primary derived fibroblasts and tumor cell lines (Fig. 3.3 A & B, respectively).

To test whether IL-17D can directly inhibit viral replication or progression, we infected either parent or IL-17D-expressing tumor cell lines. Expression of IL-17D in vitro did not protect cells from infection with VV, suggesting that IL-17D's role in protecting the host from viral infection may require the immune system. To show that the Nrf2-IL-17D pathway is induced in viral infection in vivo, we scarified WT mice with VV. Tissue harvested from mice scarified with VV had increased expression of IL-17D and Nrf2 (Fig. 3.3 C & D; example of VV scar Supplemental Fig 3.3 A & B). To model the local activation of Nrf2 and IL-17D in vivo, we adapted a system in which we topically apply tBHQ to mice[90]. Mice treated topically with tBHQ had increases in the transcript and protein levels of IL-17D and Nrf2 commensurate with those observed following infection by scarification (Fig. 3.3 D & E). Together, these results suggest that the Nrf2-IL-17D regulatory axis is activated during primary tumorigenesis and viral infection in order to confer protection to the host from disease progression.

IL-17D protects the host from primary tumorigenesis and viral infection.

It is well documented that Nrf2 protects the host from primary tumor development[91,92]. As our findings here implicate a role for the Nrf2-IL-17D regulatory axis during primary tumorigenesis, we hypothesized that IL-17D may be a critical in initiating tumor immunosurveillance programs, just as is Nrf2. To determine if IL-17D is required for tumor surveillance, we compared the development of primary tumors in WT versus IL-17D$^{-/-}$ animals, each treated with the carcinogen 3-MethylCholanthrene (MCA).

The IL-17D$^{-/-}$ mouse was obtained from the UC Davis MMRC (https://www.mmrrc.org/). We backcrossed the KO mouse fully to C57BL/6 before immunophenotyping. An analysis of major immune populations in the spleen, lymph node, and bone marrow revealed no differences in WT compared to IL-17D$^{-/-}$ mice (Fig 3.5). Additionally, we saw no differences between WT and IL-17D$^{-/-}$ in the circulating immune populations of blood (not shown). Strikingly, we observed that IL-17D$^{-/-}$ mice were significantly more susceptible to the development of primary tumors (Figure 3.4 A). Induced with a higher 25μg dose of MCA, approximately twice the number of IL-17D$^{-/-}$ mice compared to WT mice developed primary tumors. Induced with a lower 5μg dose of MCA, where WT mice are capable of full protection from primary tumor development, approximately 40% of IL-17D$^{-/-}$ mice developed primary tumors. These findings confirm that, similar to Nrf2, the cytokine IL-17D can protect the host from primary tumor formation.

ROS are key features of viral infections and regulators of ROS - particularly Nrf2 – have tremendous influence over viral pathogenesis by indirectly controlling ROS levels, which initiate and potentiate downstream antiviral immune responses[3,93,94]. However, it is unclear whether Nrf2 can directly initiate a protective immunosurveillance program. We hypothesized that Nrf2 will induce IL-17D to initiate antiviral surveillance and immunity. Following infection of WT and IL-17D$^{-/-}$ animals, we observed a delay in the resolution of the vaccinia scar in IL-17D$^{-/-}$ animals compared to WT animals at two doses of VV (Fig. 3.4 B). In a fashion similar to the role of IL-17D in host antitumor immunosurveillance, these findings suggest that virus infection-associated ROS may activate the Nrf2-IL-17D axis to initiate surveillance and contribute to host antiviral defense.

Activating Nrf2 delays tumor growth in vivo via activation of innate immunity.

Having shown a requirement for IL-17D in effective tumor surveillance[84,85], we hypothesized that Nrf2 activation in vivo would induce IL-17D in established tumor, which in turn would initiate protective immunosurveillance (Fig 3.6). To examine this, tumor bearing mice were treated topically with tBHQ or lanolin control cream beginning when tumors achieved an average diameter of 3mm, a size at which we considered them established solid tumors. In 3 out of 3 cell lines tested, we found that topical treatment with tBHQ delayed tumor growth in WT mice (Fig 3.6 A).

To determine whether the immune system was required for the antitumor effect of Nrf2 agonists, we transplanted B16 melanoma cells into immune-deficient mice *rag2*$^{-/-}$, which lack adaptive immunity but possesses intact NK cells and macrophages; *rag2*$^{-/-}$x IL2Rγ^{null} (*rag*xγ), which lack adaptive immunity as well as NK cells; and NOD-*scid* IL2Rγ^{null} (NSG) mice, which are severely immunodeficient and lack NK cells and adaptive immunity[95]. Notably, we found that topical treatment of tumors with tBHQ delayed tumor growth in *rag2*$^{-/-}$ but not *rag*xγ or NSG mice (Fig 3.6 C). To identify the immune cells activated by tBHQ treatment, we harvested treated tumors after 7 days of treatment and performed a FACS analysis of tumor infiltrating leukocytes (TILs). Our TIL analysis revealed an increase in the number of infiltrating NK cells (Fig 3.6 I). No other TIL populations were found to be different in treated versus untreated tumors (data not shown). Altogether, our results suggest that NK cells are required and sufficient to mediate Nrf2's antitumor effects.

Nrf2 agonists promote tumor rejection by activating IL-17D in tumor cells.

Recognizing that tBHQ can induce Nrf2 in both host and tumor cells and that Nrf2 could induce targets other than IL-17D, we wanted to examine: first, whether tBHQ is activating Nrf2 and IL-17D in transformed tumor versus host cells; and, second whether tBHQ necessarily induces IL-17D to mediate tumor regression. Therefore, we transplanted $Nrf2^{-/-}$ and $IL\text{-}17D^{-/-}$ mice with B16 and treated with tBHQ. We observed delayed tumor growth of B16 in both $Nrf2^{-/-}$ and $IL\text{-}17D^{-/-}$ mice (Fig 3.6 D/E), suggesting that host expression of Nrf2 and IL-17D is not required for response to tBHQ.

We next endeavored to identify a role for IL-17D in tBHQ-induced tumor rejection. To begin, we first determined whether treatment of B16 tumors with tBHQ induced IL-17D coincident with delayed tumor growth. We found that tBHQ treatment indeed led to an increase in IL-17D expression in tumors in vivo (Fig. 3.6 H). To demonstrate that IL-17D is necessary for tumor growth delay downstream of tBHQ, we created a model system in which both tumor and host would be depleted in IL-17D. To achieve an IL-17D-depleted environment, we utilized an MCA sarcoma cell line that we generated from an $IL\text{-}17D^{-/-}$ host; we named this $IL\text{-}17D^{-/-}$ MCA-sarcoma line, F38K1 (see MCA experiment in Fig 3.4). Based on established definitions for tumor growth phenotypes[62], we classify F38K1 as a progressor tumor. We confirmed F38K1's sensitivity to Nrf2 activation by stimulating the cell line in vitro and measuring HMOX-1 transcript expression, which increased in the presence of tBHQ. In vivo, tBHQ treatment of F38K1 tumors transplanted into $IL\text{-}17D^{-/-}$ mice failed to delay tumor growth (Fig 3.6 G). Additionally, tBHQ treatments in WT mice transplanted with F38K1 failed to delay

tumor growth in vivo (Fig 3.6 F). This finding implies that the antitumor response resulting from the activation of Nrf2, via topical application of tBHQ, requires tumor-expressed IL-17D and not the many previously described targets of Nrf2[68,69]. Furthermore, these results suggest that re-activating features of stress in established tumors can initiate immunesurveillance to delay tumor growth in vivo.

DISCUSSION

We have demonstrated an obligate role for IL-17D in effective tumor surveillance, optimal antiviral responses, and cancer immune therapy via Nrf2 agonists. It is well established that immune responses to viruses and transformed cells have overlapping features[6]: both involve NK cells, Th1 immunity, and CD8+ T cells. Moreover, NKG2D ligands are induced by viral infection[4,10] as well as being constitutively expressed on cancer cells[49,61]. As such, our finding that IL-17D is induced by viral infection and expressed constitutively by immunogenic cancer cells has precedence in principle and data. It is not clear what aspect of the viral infection induces IL-17D, and future experiments will examine whether TLR, NLR, and/or RLR pathways induce IL-17D.

We have definitively shown that Nrf2, an oxidative stress response factor, directly induces IL-17D and thus functions as a tumor suppressor. This role for Nrf2 is supported by previous studies showing that mice genetically deficient in Nrf2 are more susceptible to a wide range of carcinogen-induced cancers (see review [96]). For example, *nrf2*$^{-/-}$ mice displayed increased incidence of forestomach cancer and bladder cancer induced by carcinogens known to induce oxidative stress. *nrf2*$^{-/-}$ mice also had increased skin cancer

in a model of sulforaphane-mediated protection from DMBA/TPA induced carcinogenesis. To our knowledge, there are no studies to address whether Nrf2 participates in tumor immunosurveillance in any of these model systems. Importantly, cancer immunoediting and tumor elimination have been extensively documented in mouse models of MCA-induced sarcomas, and it was recently shown that MCA can acutely induce Nrf2 and its target genes[97], thus supporting our hypothesis that the Nrf2-IL-17D pathway can mediate tumor surveillance.

In contrast to the tumor suppressor role of Nrf2, other studies have shown that Nrf2 expression in tumor cells can promote their survival in the face of oxidative stress, hypoxia, and/or chemotherapy[80,91]. In fact, Nrf2 blockade has become a novel anti-cancer approach, since certain cancer cells (and model systems) report oncogene-induced, constitutive Nrf2 activity as associated with tumor growth and metastasis[98,99]. These studies have prompted a re-evaluation of the role of Nrf2 in cancer and support a model whereby Nrf2 is a "double-edged sword" that can suppress or promote cancer. Notably, a recent study found that Nrf2 acts early in tumorigenesis to suppress tumor formation and later on to promote tumor formation[100]. These results are consistent with the hypothesis that Nrf2 could induce anti-carcinogen and tumor immunosurveillance pathways in nascent tumors; but, later, protect tumor cells from oxidative stress once the transformed cells have escaped immune destruction, thereby promoting tumor progression. We speculate that the endogenous function of IL-17D could be to alert immune cells of cellular stress. Although stress ligands such as NKG2D ligands can target a cell for immune clearance, it is not clear how immune cells are recruited to sites of endogenous cellular stress. IL-17D could be one of many cytokines that participate in initiating the

"sterile inflammation," which helps to clear stressed or transformed cells. Our finding that Nrf2 also regulates IL-17D creates a novel paradigm shift whereby sterile inflammation, tumor surveillance, and oxidative stress could be linked via an Nrf2-IL-17D-NK cell pathway (Fig. 3.7).

We also found that IL-17D is induced by viral infection and is required for optimal antiviral responses. In fact, the IL-17 family of cytokines has been characterized as essential to antimicrobial host defense (see reviews [101-104]). Specifically, IL-17C and IL-17A/F are thought to mediate anti-bacterial and anti-fungal responses via recruitment of neutrophils. IL-17E contributes to anti-helminth responses via recruitment of eosinophils. Our finding that IL-17D is induced during viral infection, recruits NK cells, and is required for optimal responses to VV infection, suggests that the IL-17 family may have evolved to mediate distinct and specific anti-pathogen responses (Fig. 3.7). Given the ancient origin of the IL-17 family, it is tempting to speculate that IL-17D and IL-17C were the first family members to evolve to mediate local control of pathogen infection prior to the evolution of adaptive immunity. Future experiments will characterize the gene expression profile of cells treated with IL-17D and in particular whether it induces antiviral genes similar to how IL-17C induces antimicrobial peptides such as defensins [63]. These findings would strengthen our hypothesis that IL-17D evolved for antiviral responses.

How is oxidative stress related to carcinogenesis and viral infection? Constitutive activation of the Nrf2-IL-17D pathway in immunogenic cancer cells suggests that cancer cells undergo chronic oxidative stress, perhaps mediated to reactive oxygen species (ROS). Indeed, it was first documented in 1988 that elevated intracellular H_20_2 and tumor

progression were linked[105]. Later, Szatrowski et al discovered that human tumor cell lines produce H_20_2 at a rate comparable to that observed in PMNs[106], prompting the hypothesis that tumor-derived ROS can promote tumorigenesis and cancer progression. Soon after, work supported this hypothesis with the identification of additional cellular sources of ROS that exacerbate malignant transformation[107] and that engineering mutations to induce greater ROS production in tumor cells increased ROS-dependent metastatic potential[108]. Now, it is appreciated that a key feature of cancer cells are high levels of oxidative stress coincident with increased antioxidant defense mechanisms[1]. Our finding that certain human cancers co-express Nrf2 and IL-17D suggests that chronic oxidative stress in tumors may mediate immune surveillance, encouraging our efforts to develop therapies that can augment oxidative stress responses and promote antitumor immunity. We advocate that Nrf2 agonists already used clinically for various disease states can find "off-label" utility as immune therapies for cancer.

ROS can also be generated during viral infection, either indirectly via the superoxide burst in immune cells or directly by the virus itself. For example, viral replication and the components involved in replication can induce the generation of ROS, increasing the virulence of infection in certain instances[3,93,94]. The role of ROS in controlling viral progression in infection is unclear in all cases. While some reports show that phagocyte-derived NO is effective as an antiviral factor for DNA viruses and some RNA viruses, other reports show that ROS afford no protection against infection with viruses such as ortho/paramyxoviures, vaccinia virus, coronavirus, lymphocytic choriomeningitis virus, and murine encephalomyocarditis virus[3]. In some instances ROS can actually promote viral infections by simultaneously providing pressure for the

selection of virulent viral strains in vivo while suppressing antiviral immunity. Thus, it will be important to test the different Nrf2 agonists for efficacy in antiviral therapy. We have implicated that Nrf2 agonists, some of which are currently in clinical trials, would be highly efficacious inducers of cancer immunosurveillance and immune therapy. This mechanism of surveillance relies upon the induction of IL-17D in the tumor cells. Intriguingly, since many tumor cells downregulate IL-17D expression, it is possible that uncoupling Nrf2-IL-17D may be a mechanism of tumor escape. We have not found evidence for this mechanism, but it will be important to determine the intactness of the Nrf2-IL-17D pathway as a biomarker for responsiveness to Nrf2 agonist therapy. Moreover, whether these agonists can be used to treat a broad range of established human tumors and/or prevent the development of cancer will be an area of intense investigation. It will be important to cast a broad and deep net in these studies, as it is likely that the role of the Nrf2-IL-17D pathway in tumor progression is context dependent. Notably, the clinical use of antioxidants to prevent cancer and promote overall health may inadvertently limit an endogenous tumor surveillance pathway. On the other hand, judicious use of oxidative species may find a niche in immunotherapy. Finally, drugs such as tBHQ, which do not induce ROS but can directly induce the Nrf2-IL-17D pathway may have even higher efficacy as they would activate an endogenous tumor surveillance pathway without producing genotoxic ROS.

Chapter 3, in full, is an adapted version of the material as it appears in The Journal of Immunology, 2011, Schreiber, Robert D.; Bui, Jack D.; The American Association of Immunologists, Inc. The dissertation author was the first author of this paper.

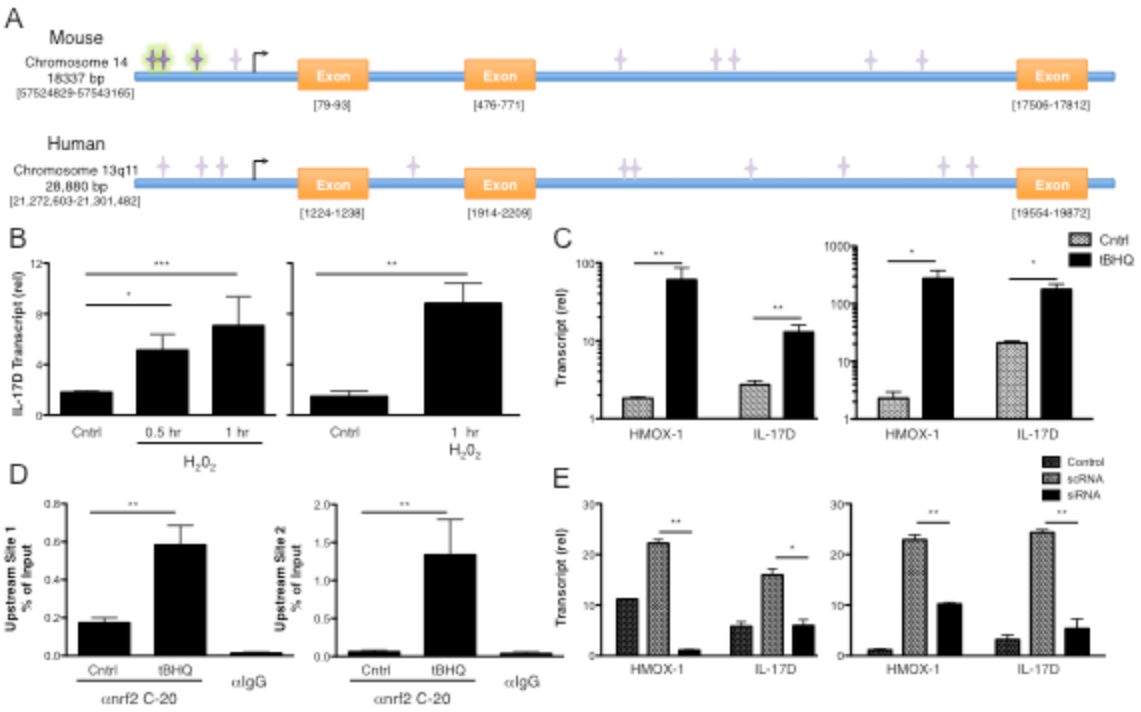

Figure 3.1 Transcription factor Nr2 induces IL-17D. (A) Consensus sequence analysis of Nrf2 tfbs in the promoter and intronic regions of human and mouse IL-17D genes. (B) H_20_2 activates Nrf2 and induces IL-17D in MEFs (left) and an MCA-induced sarcoma (right). (C) Similarly, pharmacologic activation of Nrf2 with tBHQ induces IL-17D in the murine melanoma B16 (left) and human Burkitt's Lymhoma cell line Ramos (right) (D) ChIP of B16 melanoma cells treated with tBHQ show that Nrf2 directly binds to chromatin upstream of the IL-17D gene (regions around 4196,4860, and 3730 bp upstream of the IL-17D start site). Values are expressed as the % of Nrf2 bound in immunoprecipated samples compared to input samples. (E) siRNA to Nrf2 prior to activation with H202/tBHQ in tumor cell lines blocks the induction of IL-17D [MCA sarcoma (left) or B16 melanoma (right)]. Abbreviations: tfbs [transcription factor binding site]; tBHQ [tert-butylhydroquinone]; ChIP [Chromatin immunoprecipitation]. * $P < 0.05$, ** $P < 0.01$, *** $P < 0.001$. Error bars are represented by ± SEM.

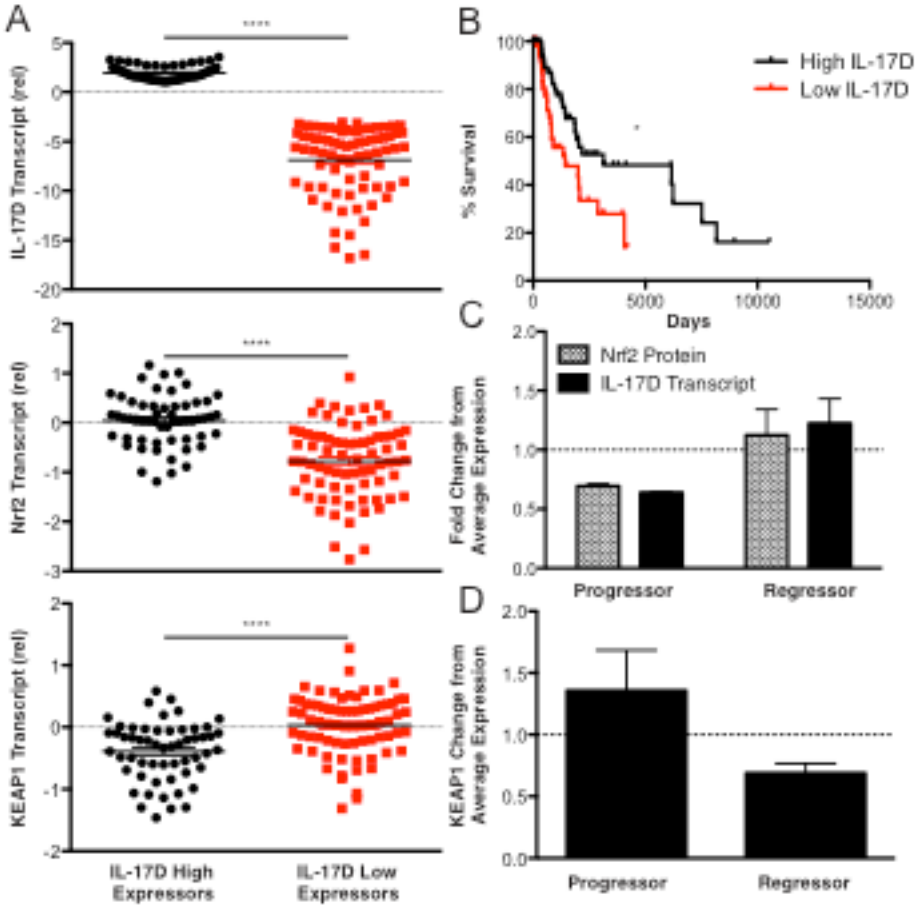

Figure 3.2 The expression of IL-17D and Nrf2 correlate with survivial in human and tumor progression in mice. (A) Human melanomas were grouped according to their expression of IL-17D into high and low expressor groups (top). High expression of IL-17D correlated with increased expression of Nrf2 (middle) and decreased expression of KEAP1 (bottom). (B) Moreover, high expression of IL-17D in patients' melanomas approximately doubled patient survival. The results shown in (A) and (B) are based in whole on data generated by the TCGA Research Network: http://thecancergenome.nih.gov/ (C) MCA-induced sarcomas grouped according to their growth phenotypes in WT mice show correlations in their expression of *il17d* transcript and Nrf2 protein. (D) KEAP1 transcript expression is inversely correlated to *il17d* and *nrf2* in MCA sarcomas grouped by growth phenotypes. * $P < 0.05$, *** $P < 0.001$. Error bars are represented by ± SEM.

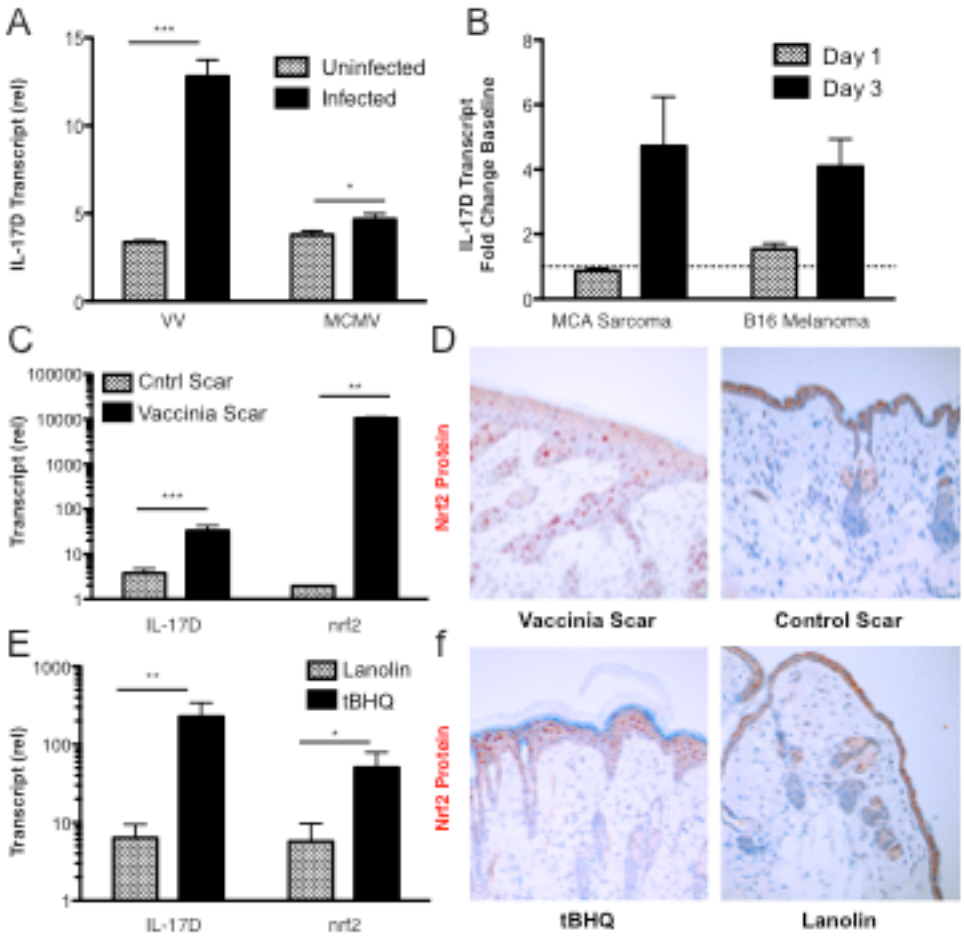

Figure 3.3 The expression of IL-17D and Nrf2 correlate during viral infection. (A) Primary-derived adults fibroblasts infected with vaccina virus (VV) or mouse cytomegalovirus (MCMV) show an increase in the transcript of IL-17D. (B) Similarly, an MCA sarcoma cell line or B16 melanoma cell line increase IL-17D transcript following viral infection in vitro. (C) Infection by scarification with VV in vivo led to an increase in IL-17D and Nrf2 transcript expression. (D) IHC for Nrf2 protein in infected versus non-infected scars show an increase in Nrf2 protein expression in skin spanning dermis to epidermis. (E) Topical application of tBHQ on the flank in vivo increased IL-17D and Nrf2 transcript expression. (f) Nrf2 protein expression was similarly increased following tBHQ topical applications. * $P < 0.05$, ** $P < 0.01$, *** $P < 0.001$. Error bars are represented by ± SEM.

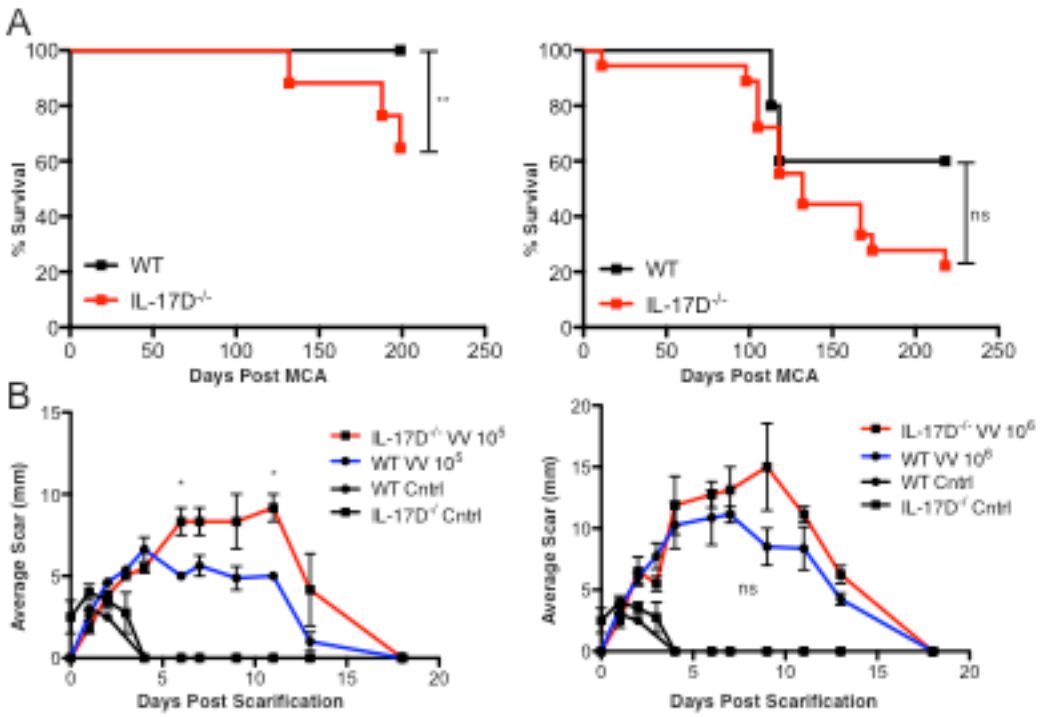

Figure 3.4 IL-17D protects from primary tumorigenesis and viral infection. (A) Primary tumors induced with the carcinogen 3-MCA in IL-17D-/- versus WT mice develop at a higher frequency at low (5mg, left) and high doses (25mg, right) of carcinogen. (B) Scars infected with VV in IL-17D-/- mice were larger than in WT before scar resolution at both a lower (10^5, left) and higher pfu (10^6, right) of virus inoculated during scarification. * $P < 0.05$, ** $P < 0.01$ Error bars are represented by ± SEM.

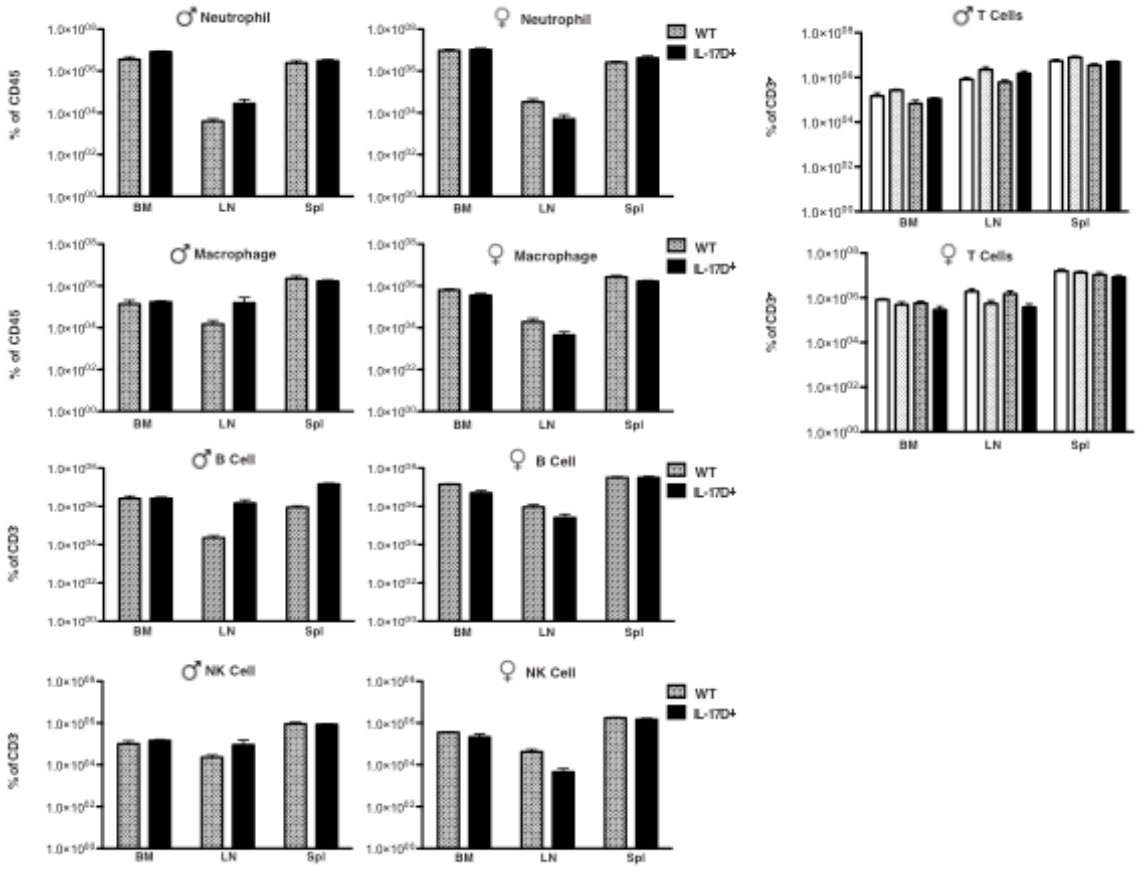

Figure 3.5 IL-17D$^{-/-}$ mouse immunophenotyping. Immunophenotyping IL-17D-/- mice show no baseline deficiencies.

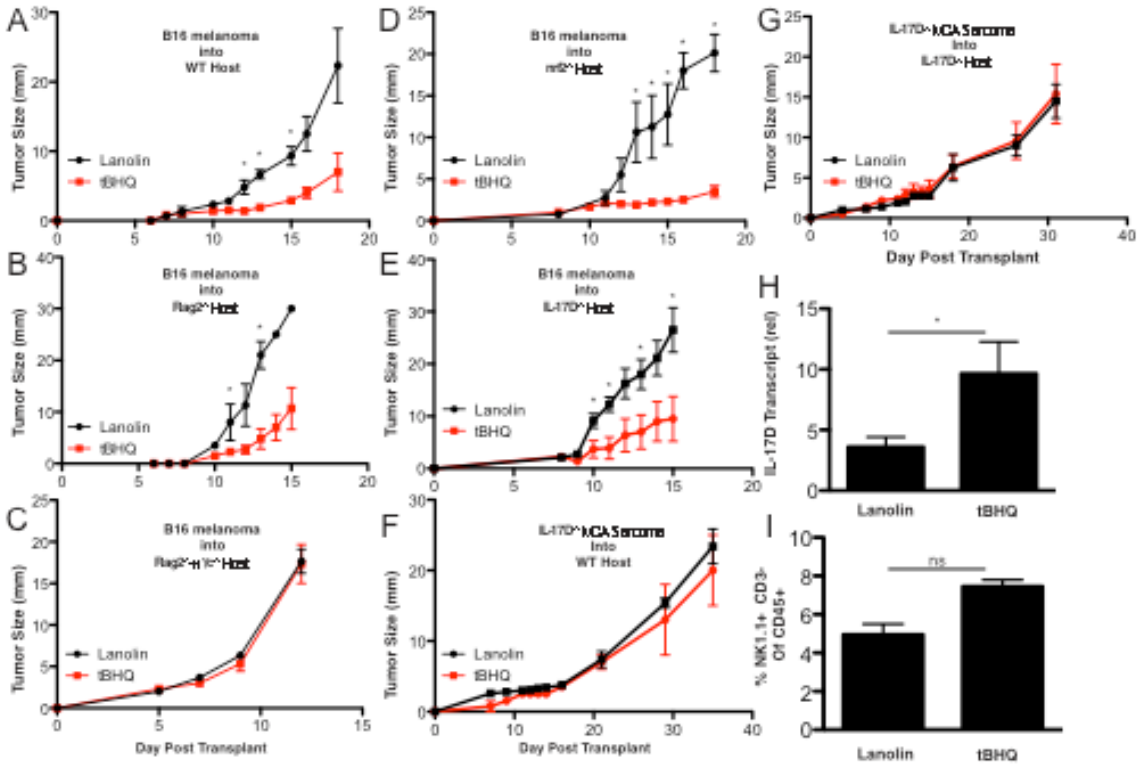

Figure 3.6 Activating Nrf2 will induce IL-17D and delay tumor growth in vivo. B16 melanoma cells (A-E) or *il17d*$^{-/-}$ MCA sarcoma cells (F-G) were transplanted subcutaneously and allowed to reach an established size (~3x3mm) before the initiation of topical treatments with tBHQ. Tumor-bearing mice were topical treated with tBHQ once daily for seven days. (A-B) When transplanted into WT (A) or *Rag2*$^{-/-}$ (B) hosts B16 regressed following topical treatments with tBHQ. (C) However, no delay in B16's growth was noted following tBHQ treatments when the tumor was transplanted into *Rag2*$^{-/-}$ x $\gamma c^{-/-}$ mice. (D-E) Topical treatments with tBHQ did delay the growth of B16 when transplanted into *nrf2*$^{-/-}$ and *il17d*$^{-/-}$ mice. (F-G) Topical tBHQ failed to induce the regression of *il17d*$^{-/-}$ MCA sarcoma cells transplanted into WT mice (F) or *il17d*$^{-/-}$ mice (G). (H) B16 tumors freshly harvested following topical treatments with tBHQ have increased transcript expression of IL-17D (I) and increased infiltration of NK cells * $P < 0.05$, ** $P < 0.01$, *** $P < 0.001$. Error bars are represented by ± SEM.

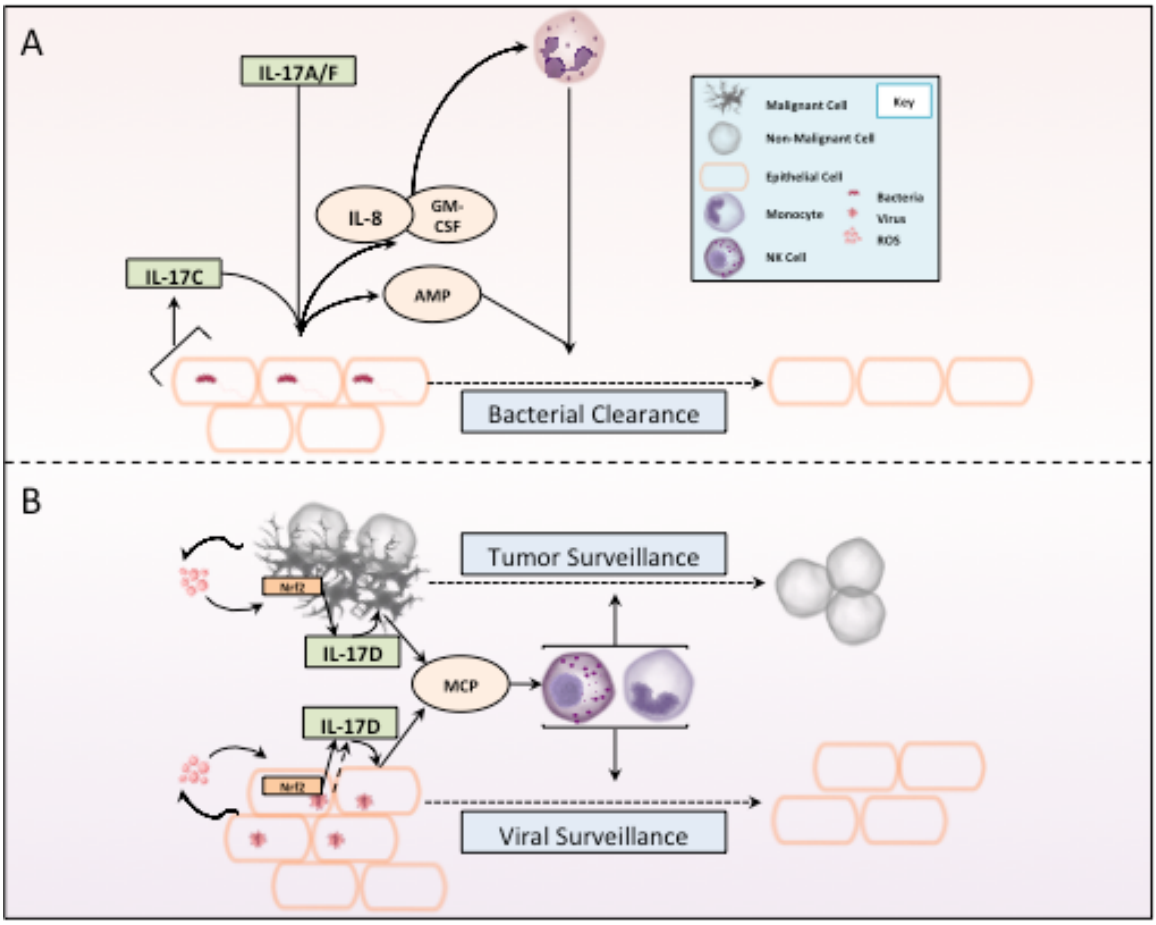

Figure 3.7 Proposed model for the primary functions of various IL-17 family members. (a) Previous work has demonstrated how IL-17A/F and IL-17C collaborate to recruit neutrophils to the site of inflammation. Distally-produced IL-17A and IL-17F and locally produced IL-17C induce the production of cytokines and chemokines from epithelium, which leads to neutrophil recruitment and Th1 type immunity. This IL-17A/F/C coordinated immune activation helps in the clearance of bacterial and fungal infections. (b) In a similar fashion to IL-17C we propose that IL-17D is induced and responds locally to recruit immune effector cells. IL-17D is induced as an early feature of the cellular response to oxidative stress common during malignant transformation and viral infection. By inducing paracrine production of chemokines, IL-17D leads to the recruitment of NK cells which assist in the clearance of virally-infected cells and malignantly transformed cells.

MATERIALS AND METHODS

All experiments involving mice were conducted under animal protocols approved by the Washington University Animal Studies Committee and the University of California, San Diego Institutional Animal Care and Use Committee (IACUC protocol #S06201) and were in accordance with ethical guidelines determined by the Peter Mac Animal Experimental Ethics Committee.

Mice and MCA induction.

Tumor induction by MCA was performed as previously described [18,55]. Briefly, cohorts of C57BL/6-strain WT (Taconic Farms), $RAG2^{-/-}$, $RAG1^{-/-}$, $IFNAR^{-/-}$, $RAG2^{-/-}$ x $STAT1^{-/-}$, and $RAG2^{-/-}$x $\gamma c^{-/-}$ mice were injected with MCA dissolved in peanut oil at various doses. Experiment 1 was performed in St. Louis and used $RAG2^{-/-}$x $\gamma c^{-/-}$ mice generated by breeding IL-2R$\gamma c^{-/-}$ mice (C57/BL6 N10+1F7-strain, Jackson Laboratories, San Diego, CA) to C57BL/6 $RAG2^{-/-}$ mice (Taconic Farms, Germantown, NY). Genotyping was performed using PCR (for IL-2Rγ_c, Jackson Labs protocol, http://jaxmice.jax.org/strain/003174.html) or by Southern blot for RAG2. Genomic microsatellite analysis showed that the $RAG2^{-/-}$x $\gamma c^{-/-}$ mice contained C57BL/6 markers at 97% of the loci tested (3% 129/Sv markers).

To control for inter-institutional breeding, minor strain differences, and housing variability,the $RAG2^{-/-}$ mice used in MCA experiment 1 were outcrossed from ($RAG2^{-/-}$x

$\gamma c^{-/-}$) x $RAG2^{-/-}$ breeding performed in-house. Tumors in mice were measured as described [18,39]. In experiment 1, a dose of MCA was used such that all MCA-treated mice developed tumors. Experiment 2 was performed at the Peter Mac facility in Australia and used $RAG2^{-/-}$x $\gamma c^{-/-}$ mice provided by WEHI (Bundoora) and C57BL/6 and $RAG1^{-/-}$ mice. To rule out that $RAG2^{-/-}$x $\gamma c^{-/-}$ tumor cell lines were rejected based on minor strain differences, we also transplanted $RAG2^{-/-}$x $\gamma c^{-/-}$ regressor cell lines into F1 (C57BL/6 x 129) mice (n=30) (Taconic Farms) and obtained identical growth patterns as in C57BL/6 mice (NCI-Frederick Rockville, MD). For some tumor transplantation experiments, $RAG2^{-/-}$x $\gamma c^{-/-}$ recipient mice were purchased from Taconic Farms. No differences in tumor growth were observed in $RAG2^{-/-}$x $\gamma c^{-/-}$ recipient mice purchased from Taconic Farms or bred in-house.

We discovered in the process of routine genotyping of our mice for the current study that the $RAG2^{-/-}$ 129/Sv mice previously obtained from Taconic Farms (RAGN12 model) and used in our 2001 publication [18] contained the C57BL/6 NK-C locus. Microsatellite analysis confirmed that these mice were virtually congenic at the NK-C locus and contained approximately 22 cM of C57BL/6 sequence encompassing the following genes/markers: D6MIT261, D6MIT105, D6MIT018, D6MIT111, Nkrp1a, Nkrp1c, CD69, Nkg2d, Nkg2a, and Ly49a. These mice were therefore designated 129/SvEv.cNK-C.B6 $RAG2^{-/-}$ mice.

Since the NK-C gene locus displays allelic polymorphism and can contribute to part of the difference in NK cell activity between the C57BL/6 and 129/Sv strain,new sets of MCA-induced sarcomas were generated using $RAG2^{-/-}$ mice that had been bred by Taconic Farms to be on a pure 129/SvEv background (129S6/SvEvTac-*Rag2*^{tm1Fwa}). This

new set of MCA-induced sarcomas was published in reference 27 and further studied in Figure 3.

Cell Lines.

MCA-induced sarcoma cell lines were generated from primary tumors (see methods MCA Primary Tumorigenesis) and expanded in vitro until at least the second passage before freezing. For experimentation tumor cell lines were thawed from early passages and grown in RPMI 1640 (Gibco) supplemented with 10% FCS (Atlanta Biologics) (as previously described[62]). Other tumor cell lines used – Ramos, B16, LLC – were cultured similarly. Primary derived mouse embryonic fibroblasts were derived from fetuses 12.5-13.5 days p.c. (as described[109]).

Nrf2 Activation and Knockdown

Nrf2 was activated in cell lines in vitro with either tert-butylhydroquinone (Spectrum) or H_20_2 (Fisher). tBHQ was used at 50mM in DMSO, and H_20_2 was used at 10mM for 0.5-1 hours before being washed out. Treated cells were harvested at timepoints between 6 and 12 hours for analysis. Activation of Nrf2 in vivo was adapted from methods described by Schafer et al[110]. For in vivo Nrf2 activation a cream containing 50mM tBHQ solubilized in DMSO was mixed 1:1 (v/v) with Lanolin cream (Sigma) and heated gently in a water bath to allow for mixing. The mixture, poured into sterile dishes (Falcon), was allowed to cool overnight before use in vivo. Hair along the flank was removed one day before the

initiation of topical treatments. Control topical treatments consisted of a 1:1 mixture of DMSO:Lanolin. To knockdown Nrf2, a mixture of three siRNAs to nrf2 or control siRNA were used (Invitrogen)[111]. siRNA was transfected into cells with Lipofectamine 2000 (Thermo Fisher) as recommended by the manufacturer (http://www.lifetechnologies.com/).

Transcription Factor Binding Analysis

Sequences for mouse and human *il17d* genes were analyzed for the presence of antioxidant responsive elements (ARE) [TGAcTCAGCa], a sequence to which the Nrf2-sMAF heterodimer is known to bind[81].

The Cancer Genome Atlas (TCGA)

Human tumor data was sourced from the TCGA analytical tool, UCSC Cancer Genome Browser (http://cancergenome.nih.gov/). PANCAN normalized gene expression data was used to partition tumors into roughly equally numbered groups, compare transcript expression levels, and generate survival curves for patients.

Tumorigenesis and Transplantations.

Primary tumorigenesis was performed as previously described[18,62]. 3-MethylCholanthrene was dissolved in corn oil (Sigma) prior to instillation. To induce

primary tumors, 5mg or 25mg doses of MCA were injected subcutaneously along a single flank of C57BL/6-strain WT or *il17d*$^{-/-}$ mice. Tumor development was monitored and measured weekly between two and six months post MCA instillation. Tumors were harvested for cell line generation, FFPE blocks, TILs and RNA when tumors achieved an average diameter of 25mm. For transplantation studies tumor cell lines were trypsinized, washed with cold PBS three times, and injected subcutaneously along the flanks of mice (previously described[62]). Hair was removed from the flanks of mice at least one day prior to transplantation. Tumor progression was assessed by averaging the greatest two diameter measurements of the tumor.

Microarray and Clustering Analysis.

Using transplantation assays, we reported that all of the tested 17 primary fibrosarcomas from wild type mice were poorly immunogenic and formed progressively growing tumors in immunocompetent naïve hosts when 1 x 10^6 cells were injected subcutaneously[1]. We designated those as WT tumors and randomly selected 8 (H128m, d4m3, F279, H118, F236, d22m1, F244, and d22m2) for microarray analysis. Sixty percent (12/20) of the RAG2$^{-/-}$ mice-derived tumors also formed progressively growing tumors in naïve host[1]. We designated those as RAG2$^{-/-}$ progressors and selected 8 (d29m1, F221, d57, d53, d30m1, d28m3, H50, and H52) randomly for analysis. In contrast, 40% (8/20) of RAG2$^{-/-}$ mice-derived tumors were significantly more immunogenic and were rejected in immunocompetent naïve mice even at high dose inoculation of tumor challenge[1]. We designated those as RAG2$^{-/-}$ regressors and 8 (d38m2, F510, F535, d42m1,

F515, H31m1, d27m2, and d30m4) were used in analysis. Tumor cells were thawed and cultured for 4 or 5 days, and total RNA was extracted using Trizol reagent (Invitrogen, Carlsbad, CA) and prepared using the RNA-Bee protocol (Tel-Test, Friendswood, TX). With 20mg of total RNA, cDNA was synthesized by Super Script Choice System (Gibco BRL Life Technologies, Grand Island, NY) with T7-(dT)24 Primer (Genset Corp, San Diego, CA), and was cleaned up by Phase Lock Gels (Eppendorf-5 Prime, Inc., Boulder, CO) with Phenol/chloroform/isoamyl alcohol (Ambion, Grand Island, NY). Biotin-labeled cRNA was synthesized by BioArray HighYield RNA Transcript Labeling Kit (Enzo, Farmingdale, NY), and cleaned up by RNeasy Mini Kit (Qiagen, Valencia, CA). Murine Genome U74v2 Set GeneChip Arrays (Affymetrix, Santa Clara, CA) were hybridized with Biotin-labeled cRNA with GeneChip Hybridization Oven 320 (Affymetrix, Santa Clara, CA), and washed and stained with GeneChip Fluidics Station 400 (Affimetrix, Santa Clara, CA). Gene signals were scanned by GeneArray Scanner (Hewlett Packard, Palo Alto, CA), and differential expression data was analyzed on Microarray Suit Software (Affymetrix, Santa Clara, CA). Data was normalized, statistically analyzed, and clustered by DecisionSite for Functional Genomics (Spotfire, Somerville, MA).

Generation of IL-17D deficient and overexpressing tumor cell lines.

Daughter ctrl and sh17D regressor tumor cell lines were generated by transducing parental regressor tumor cell lines with either a retrovirus-expressing scramble sequence (shctrl) or retroviruses expressing shRNA's specific for the 3'UTR and coding sequence

of IL-17D and selected on puromyocin supplemented media for 1 week. Daughter ctrl and ex17D progressor tumor cell lines were generated by either transducing parental progressor tumor cell lines with an empty vector lentivirus (ctrl) or a lentivirus-expressing IL-17D cDNA and selected on blastocydin supplemented media for 1 week. Conditional expressing IL-17D daughter progressor tumor cell lines were generated by transducing parental F244 progrssor tumor cell line with a lentivirus-expressing the tet repressor and selected on blastocydin for 1 week. Resulting cells were then trasnduced with a lentivirus-expressing IL-17D regulated by the tet operator sequence and selected on puromyocin supplemeted media for 1 week.

Antibodies and FACS analysis.

On various days post-transplantation, tumors were excised from mice, minced, and treated with 1 mg/mL type IA collagenase (Sigma) as described (1). Cells were vigorously resuspended, washed in FACS buffer (PBS+1% FCS+0.05%NaN_3, Sigma) and filtered before staining. Antibodies to CD45, F4/80, NK1.1, CD69, CD80, CD206, Ly6C, CD11b, I-A/I-E , 1A8, and steptavidin PE were from BD PharMingen (San Diego, CA). Staining was conducted for 15-20 minutes at 4º in FACS tubes containing 1-2 million total cells, 0.5-1 ml of antibody, 1 ml of FC block (anti-CD16/32), and 100 ml of FACs buffer. 7AAD (Calbiochem) or Propidium Iodide (Sigma) was added at 1 mg/mL immediately prior to FACS analysis. M1-type and M2-type macrophages were gated as published [33]. Cells were harvest with dPBS or HBSS supplemented with 2.5 mM EDTA. Trypsin was not used since it decreased NKG2D tetramer staining, presumably by

cleaving the ligands. NKG2D tetramers were generated as described (20). Monoclonal antibodies to H60a, pan-RAE-1, and MULT1 were obtained from R&D (Minneapolis, MN). Secondary antibodies were obtained from Biolegend (San Diego, CA). For intracellular IL-17D staining, cells were either incubated with or without 2μM monensin (Sigma, St. Loius, MO) and 1μg/ml Brefeldin A (BD biosciences, San Jose, CA) and then harvested by trypsinization, washed once with PBS, incubated with Cytofix (BD biosciences, San Jose, CA) for 15 min at 4^{o}, washed twice with Perm wash (BD biosciences, San Diego) solution, and anti-IL17D (R&D Systems, Minneapolis, MN) or rat IgG2a isotype control (eBioscience, San Diego, CA) monoclonal antibodies were added. Staining was conducted for 30 minutes at 4º in FACS tubes containing 0.5-2 million total cells, 0.5-1 ml of antibody, and 100 ml of FACs buffer (PBS+1% FCS+0.09% NaN_3, Sigma, St. Louis, MO). Cells were washed twice with Perm wash and then resuspended in FACS stain buffer. All analyses were done on live cells identified by forward and side scatter properties with a FACScanto II (BD Biosciences, San Jose, CA). IL-17D mean channel shift (MCS) is given as isotype staining subtracted from signal values. % Control mean channel shift (% of Ctrl MCS) is normalized to control sample mean channel shift values.

Generation of tumor cell line cDNA libraries and quantitative PCR.

Tumor cell lines were plated in triplicate at 6 x 10^4 cells/well in a 6 well plate and incubated for 48 hours at 37^{o}. Supernatant was aspirated and cells were washed twice with PBS before addition of 1ml Trizol reagent (Invitrogen, Carlsbad, CA) and RNA was

prepeared using the RNA-Bee protocol (Tel-Test, Friendswood, TX). cDNA was prepared using the Applied Biosystems protocol (Branchburg, NJ). Relative qPCR was done using IL-17D specific Taqman FAM probes (Invitrogen, Carlsbad, CA) with internal GAPDH-VIC probe controls and amplified using a 7300 Real Time PCR System (Applied Biosystems, Branchburg, NJ). IL-17D transcript was quantified relative to GAPDH expression using the equation $2^{-(\Delta Ct)}$.

Immunohistochemistry.

Fresh tumor nodules were harvested, OCT-embedded, and snap frozen in cooled isopentane. Tissue blocks were cut on a cryostat into 6 μm-thick sections, mounted onto poly-L-Lysine slides, air-dried overnight, and post-fixed for 10' in acetone before staining. Purified rat anti-mouse CD16/CD32 was used as Fc block for 20' (BD Pharmingen; dilution 1:50) when appropriate. Biotin-conjugated rat anti-mouse I-A/I-E (eBioscience; dilution 1:100, 1 hr at rt) and biotin-conjugated rat anti-mouse CD206 (Biolegend; dilution 1:100, 1 hr at rt) staining was revealed using streptavidin-HRP (Vector Laboratoies; 30 minutes at rt) followed by amino-ethyl-carbazole as chromogen (BD; 10-15min at rt). Purified rat anti-mouse CD68 (Biolegend; dilution 1:100) staining was detected using a biotin-conjugated rabbit polyclonal anti-rat IgG, mouse adsorbed (Vector; dilution 1:200). Immunostained tissue sections were examined with a Leica DM 2500 or Nikon Eclipse E800 microscope; images were captured with a Leica DFC 420 or Nikon DXM 1200 digital camera, respectively. Quantitative analysis of MHC-II$^+$, CD68$^+$,

$CD206^+$ cells was obtained by counting at least 10 high power fields (HPF) of tissue sections at 200x magnification.

Chromatin Immunoprecipitation

ChIP for Nrf2 was performed as described previously[98]. Following activation of Nrf2 with tBHQ (see Nrf2 Activation and Knockdown methods), cells were fixed in 1% formaldehyde for 10 minutes at room temperature, quenched with 0.125M glycine for 5 minutes at room temperature, washed with cold PBS and resuspended in lysis buffer [1% SDS, 10mM EDTA pH 8, 50mM Tris-HCL pH 8], fresh protease inhibitor cocktail for 5 minutes on ice. To generate chromatin fragments of around 200bp, cell lysates were then sonicated on ice for 15 cycles [15 seconds on, 45 seconds off] and pelleted by centrifugation at 13,000 rpm for 5 minutes. Protein A dynabeads (Life Technologies), pre-blocked in 0.5% BSA in PBS (w/v), were incubated with 8mg Nrf2 antibody C-20 (Santa Cruz Biotech) or normal rabbit IgG (sc-2027, Santa Cruz Biotech) overnight at 4^0C and then washed with additional blocking buffer and RIPA. To immunoprecipitate Nrf2-chromatin complexes, conjugated dynabeads were mixed with sonicated lysate - diluted 1:9 in dilution buffer with protease inhibitors - and allowed to rotate overnight at 4^0C. Immunoprecipitates were processed as suggested by the dynabeads manufacturer, Life Technologies (https://www.lifetechnologies.com/us/en/home.html) and purified using the QiaQuick PCR DNA kit (Qiagen). qPCR sequences used for ChIP samples appear in **Table 4** (see qPCR Methods).

Western Blot

Cells were lysed in 4x sample buffer containing SDS (Bio-Rad) and b-mercaptoethanol (Sigma) before boiling at 95^0C for 5 min. Samples were run on SDS-PAGE gels (Biorad), and expression of Nrf2 was analyzed by western blotting using anti-Nrf2 antibody (C-20, Santa Cruz Biotech). b-actin antibodies were used to control for differences in gel loading (A5441, Sigma-Aldrich). Blotted bands were scanned and quantified with CS6 Photoshop imaging software, and represented as fold expression of average of expression across tumor cell lines.

Cytokine Secretion Assay.

On various days post-transplantation, tumors were excised from mice, minced, and treated with 1 mg/mL type IA collagenase (Sigma). Filtered tumor/immune cell suspensions were plated in triplicate wells at 40,000 cells/well in 100 mL for 24 hrs at 37^oC. Supernatant was analyzed for cytokines using the mouse inflammation cytometric bead array kit from BD Biosciences (San Jose, CA).

Chromium release assay.

Splenocytes from RAG2-/- mice were activated by culturing in media with 1000 U/ml human IL-2 (Chiron, Emeryville, CA). Day 7 IL-2-activated NK effector cells were used in a 4-hour 51Cr release assay using tumor target cells labeled with 51Cr as described (20) with either control IgG or anti-NKG2D. Bars depict standard error of

triplicates. All experiments were done at least twice. ANOVA was used to assess statistical significance between parent and passaged cell lines.

Mouse air pouch experiments.

C56BL/6 x 129/Sv F1 mice were injected s.c with 3ml of sterilized air filtered through a 0.2μm Millipore filter (Bellerica, MA) to form air pouches on day 0 and re-inflated again on day 3. On day 7, either 1ml of LPS (1μg/ml), 1ml of rmIL-17A (5μg/ml) (R&D Systems, Minneapolis, MN), 1ml of rmIL-17D (5μg/ml) (R&D Systems, Minneapolis, MN), 1ml rmIL-17D (5μg/ml) (Mayfield Lab), 1ml of rmMCP-1 (5μg/ml) (Peprotech, Rocky Hill, NJ), or 1ml of rmIL-17D (5μg/ml) and anti-MCP-1 polyclonal antibodies (25μg/ml) (R&D Systems, Minneapolis, MN) was injected into mouse air pouches 8h before air pouch harvest. Air pouches were lavaged with 2ml PBS and centrifuges at 1250 rpm for 5 min at room temperature. Supernatant was harvested and analyzed for chemokine protein levels using the mouse chemokine flowcytomix kit from eBioscience (San Diego, CA). Infiltrating air pouch cells were resuspended in FACS stain buffer, counted on a hemocytometer, incubated with antibodies against CD45, CD4, CD8, B220, CD11c, DX5, NK1.1, MAC1, Ly6G, and I-A/I-E for 15 min at 4^{o}, washed, and resuspended in FACS buffer containing 1ug/ml 7AAD (Sigma, St Lous, MO) to identify viable cells before analysis. Total number of infiltrating immune cell subsets were calculated from percentages obtained from FACS analysis of the total cell count for each sample.

Chemokine Secretion Assay.

On days 7 and 14 post-transplantation, tumors were excised from mice, minced, and treated with 1 mg/mL type IA collagenase (Sigma, St Louis, MO) as described[6]. Filtered tumor/immune cell suspensions were plated in triplicate wells at 40,000 cells/well in 100 mL for 24 hrs at 37^{o}C. Supernatant was analyzed for chemokines using the mouse chemokine flowcytomix kit from eBioscience (San Diego, CA).

NK cell kill assay.

Splenocytes from RAG2$^{-/-}$ mice were activated by culturing in media with 1000 U/ml human IL-2 (Chiron, Emeryville, CA). Day 7 IL-2-activated NK effector cells were centrifuged with CFSE labeled tumor cell lines at varying ratios and incubated for 6h at 37^{o}. Cells were washed and resuspended in FACS buffer containing 1ug/ml 7AAD (Sigma, St Louis, MO) to identify viable cells. % Specific target lysis is given as the percentage of CFSE+7AAD+ cells by FACS analysis.

Chemotaxis assay.

In vitro chemotaxis was performed using indicated tumor supernatant or 600μl of RPMI+ 0.5% FBS supplemented with varying doses of either rmIL-17D, or 100ng/ml MCP-1 added to 24 well plates with 5um polycarbonate membrane filter added on top. 5 x 10^5 WT bone marrow cells were added in 100μl of RPMI+0.5%FBS or complete media,

added on the top of the membrane, and incubated at 37^{o} for 3h. Migrated cells were harvested by removing transwells and collecting suspended cells in the bottom well. Cells were resuspended in FACS stain buffer, incubated with antibodies against CD45, CD4, CD8, B220, CD11c, DX5, NK1.1, MAC1, Ly6G, and I-A/I-E for 15 min at 4^{o}, washed, and resuspended in FACS buffer containing 1μg/ml 7AAD (Sigma, St Louis, MO) to identify viable cells before analysis. Total viable migrating cell counts were acquired by complete sample collection under a constant flow rate and analyzed by FACS analysis.

In vitro growth assay.

Various tumor cell lines were seeded in 96 well plates at 5 x 10^3 cells in 200μl and incubated at 37^{o} and expanded when necessary. At indicated time points cells were harvested by trypsinization, washed and counted using a hemocytometer.

Statistical Analysis.

Statistical significance between two groups was determined by the Welch's t-test using two-tailed analysis to obtain p-values. The Log-Rank test was used to compare the survival of mice across tumor transplantation or induction conditions. Error bars are depicted using standard error (SEM). All experiments were done at least twice.

Viral Infections

Vaccinia Virus (VV) Western Reserve was kindly donated by the Dr. Ananda Goldrath (UCSD) and Murine Cytomegalovirus Smith Strain (MCMV) by Dr. Elina Zuniga (UCSD). MCMV salivary gland stocks were prepared by infection of four to six week old BALB/c mice with $5x10^3$ pfu i.p. After two weeks, glands were pooled and homogenized in sterile RPMI medium. Viral titers were determined by plaque assay on NIH 3T3 cells after two hours of virus absorption and five days of methylcellulose overlay. Primary fibroblasts or tumor cell lines were incubated with $1x10^5$pfu of MCMV or VV, respectively, per $4x10^5$ cells for 2h. Virus inoculum was removed, and cells were incubated for another 4h or 22h before harvesting in Trizol for later analysis. Viral titers following VV infection were determined by plaque assays on Vero cells (kindly donated by Dr. Elina Zuniga). Vero cells were incubated with viral inoculum from infected cells for one hour, washed out, and grown for two days before fixation with 4% PFA and staining with crystal violet (Sigma) to assist in the quantification of virus titers. In vivo, age and sex-matched eight to twelve week old C57Bl/6 WT or *il17d*$^{-/-}$ mice were infected with VV by scarification at $1x10^5$ or $1x10^6$ pfu. VV scars were monitored daily and expressed as the average of the two maximum scar diameters.

REFERENCES

1. Gorrini, C., Harris, I. S. & Mak, T. W. Modulation of oxidative stress as an anticancer strategy. *Nat Rev Drug Discov* **12,** 931–947 (2013).

2. Martindale, J. L. & Holbrook, N. J. Cellular response to oxidative stress: Signaling for suicide and survival. *J. Cell. Physiol.* **192,** 1–15 (2002).

3. Schwarz, K. B. Oxidative stress during viral infection: a review. *Free Radic. Biol. Med.* **21,** 641–649 (1996).

4. Eric Vivier, David H Raulet, Alessandro Moretta, Michael A Caligiuri, Laurence Zitvogel, Lewis L Lanier, Wayne M Yokoyama, and Sophie Ugolini. Innate or adaptive immunity? The example of natural killer cells. *Science* **331,** 44–49 (2011).

5. Alcami, A. & Koszinowski, U. H. Viral mechanisms of immune evasion. *Immunology Today* **21,** 447–455 (2000).

6. Raulet, D. H. & Guerra, N. Oncogenic stress sensed by the immune system: role of natural killer cell receptors. *Nature Reviews Immunology* **9,** 568–580 (2009).

7. Schreiber, R. D., Old, L. J. & Smyth, M. J. Cancer Immunoediting: Integrating Immunity's Roles in Cancer Suppression and Promotion. *Science* **331,** 1565–1570 (2011).

8. Groth, A., Klöss, S., Pogge von Strandmann, E., Koehl, U. & Koch, J. Mechanisms of Tumor and Viral Immune Escape from Natural Killer Cell-Mediated Surveillance. *J Innate Immun* **3,** 344–354 (2011).

9. Hayday, A. C. Gammadelta T cells and the lymphoid stress-surveillance response. *Immunity* **31,** 184–196 (2009).

10. Seema Shafi, Pierre Vantourout, Graham Wallace, Ayman Antoun, Robert Vaughan, Miles Stanford, and Adrian Hayday *l.* An NKG2D-mediated human lymphoid stress surveillance response with high interindividual variation. *Science Translational Medicine* **3,** 113ra124 (2011).

11. Bui, J. & Schreiber, R. Cancer immunosurveillance, immunoediting and inflammation: independent or interdependent processes? *Current opinion in immunology* **19,** 203–208 (2007).

12. Zitvogel, L., Tesniere, A. & Kroemer, G. Cancer despite immunosurveillance: immunoselection and immunosubversion. *Nature Publishing Group* **6,** 715–727 (2006).

13. Allavena, P., Sica, A., Solinas, G., Porta, C. & Mantovani, A. The inflammatory micro-environment in tumor progression: The role of tumor-associated macrophages. *Critical Reviews in Oncology/Hematology* **66,** 1–9 (2008).

14. Balkwill, F. & Mantovani, A. Inflammation and cancer: back to Virchow? *The Lancet* **357,** 539–545 (2001).

15. Coussens, L. M. & Werb, Z. Inflammation and cancer. *Nature* **420,** 860–867 (2002).

16. Balkwill, F. & Coussens, L. M. An inflammatory link. *Nature* **431,** 405–406 (2004).

17. Ben-Neriah, Y. & Karin, M. Inflammation meets cancer, with NF-κB as the matchmaker. *Nat Immunol* **12,** 715–723 (2011)

18. V Shankaran, H Ikeda, AT Bruce, JM White, PE Swanson, LJ Old, and RD Schreiber. IFNγ and lymphocytes prevent primary tumour development and shape tumour immunogenicity. *Nature* **410,** 1107–1111 (2001).

19. Dunn, G., Old, L. & Schreiber, R. The immunobiology of cancer immunosurveillance and immunoediting. *Immunity* **21,** 137–148 (2004).

20. Vesely, M. D., Kershaw, M. H., Schreiber, R. D. & Smyth, M. J. Natural Innate and Adaptive Immunity to Cancer. *Annual review of immunology* **29,** 235–271 (2011).

21. Smyth, M. J., Dunn, G. P. & Schreiber, R. D. Cancer immunosurveillance and immunoediting: the roles of immunity in suppressing tumor development and shaping tumor immunogenicity. *Adv. Immunol.* **90,** 1–50 (2006).

22. Gavin P Dunn, Allen T Bruce, Kathleen C F Sheehan, Vijay Shankaran, Ravindra Uppaluri, Jack D Bui, Mark S Diamond, Catherine M Koebel, Cora Arthur, J Michael White, and Robert D Schreiber. A critical function for type I interferons in cancer immunoediting. *Nat Immunol* **6,** 722–729 (2005).

23. Mark J Smyth, Jeremy Swann, Erika Cretney, Nadeen Zerafa, Wayne M Yokoyama, and Yoshihiro Hayakawa. NKG2D function protects the host from tumor initiation. *The Journal of experimental medicine* **202,** 583–588 (2005).

24. Shayna E A Street, Yoshihiro Hayakawa, Yifan Zhan, Andrew M Lew, Duncan MacGregor, Amanda M Jamieson, Andreas Diefenbach, Hideo Yagita, Dale I Godfrey, and Mark J Smyth. Innate immune surveillance of spontaneous B cell lymphomas by natural killer cells and gammadelta T cells. *The Journal of*

experimental medicine **199,** 879–884 (2004).

25. Crowe, N. Y., Smyth, M. J. & Godfrey, D. I. A Critical Role for Natural Killer T Cells in Immunosurveillance of Methylcholanthrene-induced Sarcomas. *Journal of Experimental Medicine* **196,** 119–127 (2002).

26. Takeda, K., Smyth, M. & Cretney, E. Critical role for tumor necrosis factor–related apoptosis-inducing ligand in immune surveillance against tumor development. *The Journal of ...* (2002).

27. Smyth, M. & Godfrey, D. A fresh look at tumor immunosurveillance and immunotherapy. *Nat Immunol* (2001).

28. Smyth, M. J., Hayakawa, Y., Takeda, K. & Yagita, H. New aspects of natural-killer-cell surveillance and therapy of cancer. *Nature Reviews Cancer* **2,** 850–861 (2002).

29. Antonio Sica, Paola Larghi, Alessandra Mancino, Luca Rubino, Chiara Porta, Maria Grazia Totaro, Monica Rimoldi, Subhra Kumar Biswas, Paola Allavena, and Alberto Mantovani. Macrophage polarization in tumour progression. *Seminars in Cancer Biology* **18,** 349–355 (2008).

30. Lewis, C. E. Distinct Role of Macrophages in Different Tumor Microenvironments. *Cancer Research* **66,** 605–612 (2006).

31. Gordon, S. Monocyte and macrophage heterogeneity. *Nature Reviews Immunology* (2005).

32. Bui, J., Carayannopoulos, L., Lanier, L., Yokoyama, W. & Schreiber, R. IFN-dependent down-regulation of the NKG2D ligand H60 on tumors. *The Journal of Immunology* **176,** 905 (2006).

33. K Movahedi, D Laoui, C Gysemans, M Baeten, G Stange, J Van Den Bossche, M Mack, D Pipeleers, P In't Veld, P De Baetselier, and J A Van Ginderachter. Different Tumor Microenvironments Contain Functionally Distinct Subsets of Macrophages Derived from Ly6C(high) Monocytes. *Cancer Research* **70,** 5728–5739 (2010).

34. Lewis, C. & Pollard, J. Distinct role of macrophages in different tumor microenvironments. *Cancer Research* **66,** 605–612 (2006).

35. Rakhmilevich, A. L., Buhtoiarov, I. N., Malkovsky, M. & Sondel, P. M. CD40 ligation in vivo can induce T cell independent antitumor effects even against immunogenic tumors. *Cancer Immunol Immunother* **57,** 1151–1160 (2008).

36. Ilia N Buhtoiarov, Hillary Lum, Gideon Berke, Donna M Paulnock, Paul M Sondel, and Alexander L Rakhmilevich. CD40 ligation activates murine macrophages via an IFN-gamma-dependent mechanism resulting in tumor cell destruction in vitro. *J. Immunol.* **174,** 6013–6022 (2005).

37. Hillary D Lum, Ilia N Buhtoiarov, Brian E Schmidt, Gideon Berke, Donna M Paulnock, Paul M Sondel, and Alexander L Rakhmilevich. Tumoristatic effects of anti-CD40 mAb-activated macrophages involve nitric oxide and tumour necrosis factor-alpha. *Immunology* **118,** 261–270 (2006).

38. O'Sullivan, T., Dunn, G. P., Lacoursiere, D. Y., Schreiber, R. D. & Bui, J. D. Cancer Immunoediting of the NK Group 2D Ligand H60a. *The Journal of Immunology* **187,** 3538–3545 (2011).

39. Catherine M Koebel, William Vermi, Jeremy B Swann, Nadeen Zerafa, Scott J Rodig, Lloyd J Old, Mark J Smyth, and Robert D Schreiber. *et al.* Adaptive immunity maintains occult cancer in an equilibrium state. *Nature* **450,** 903–907 (2007).

40. Hanahan, D. & Weinberg, R. A. Hallmarks of Cancer: The Next Generation. *Cell* **144,** 646–674 (2011).

41. Hibbs, J. B., Lambert, L. H. & Remington, J. S. Resistance to murine tumors conferred by chronic infection with intracellular protozoa, Toxoplasma gondii and Besnoitia jellisoni. *J. Infect. Dis.* **124,** 587–592 (1971).

42. Hibbs, J. & Lambert, L. Control of carcinogenesis: a possible role for the activated macrophage. *Science* (1972).

43. Pace, J., Russell, S. & Schreiber, R. Macrophage activation: priming activity from a T-cell hybridoma is attributable to interferon-gamma. in (1983).

44. Schreiber, R., Pace, J. & Russell, S. Macrophage-activating factor produced by a T cell hybridoma: physiochemical and biosynthetic resemblance to gamma-interferon. *The Journal of ...* (1983).

45. Weinberg, J. B., Chapman, H. A. & Hibbs, J. B. Characterization of the effects of endotoxin on macrophage tumor cell killing. *J. Immunol.* **121,** 72–80 (1978).

46. Kleinerman, E., Erickson, K., Schroit, A. & Fogler, W. Activation of tumoricidal properties in human blood monocytes by liposomes containing lipophilic muramyl tripeptide. *Cancer Research* (1983).

47. G L Beatty, E G Chiorean, M P Fishman, B Saboury, U R Teitelbaum, W Sun, R D Huhn, W Song, D Li, L L Sharp, D A Torigian, P J O'Dwyer, and R H

Vonderheide. CD40 Agonists Alter Tumor Stroma and Show Efficacy Against Pancreatic Carcinoma in Mice and Humans. *Science* **331,** 1612–1616 (2011).

48. Roi Gazit, Raizy Gruda, Moran Elboim, Tal I Arnon, Gil Katz, Hagit Achdout, Jacob Hanna, Udi Qimron, Guy Landau, Evgenia Greenbaum, Zichria Zakay-Rones, Angel Porgador, and Ofer Mandelboim. Lethal influenza infection in the absence of the natural killer cell receptor gene Ncr1. *Nat Immunol* **7,** 517–523 (2006).

49. Nadia Guerra, Ying Xim Tan, Nathalie T Joncker, Augustine Choy, Fermin Gallardo, Na Xiong, Susan Knoblaugh, Dragana Cado, Norman R Greenberg, and David H Raulet. NKG2D-Deficient Mice Are Defective in Tumor Surveillance in Models of Spontaneous Malignancy. *Immunity* **28,** 571–580 (2008).

50. S Gilfillan, C J Chan, M Cella, N M Haynes, A S Rapaport, K S Boles, D M Andrews, M J Smyth, and M Colonna. DNAM-1 promotes activation of cytotoxic lymphocytes by nonprofessional antigen-presenting cells and tumors. *Journal of Experimental Medicine* **205,** 2965–2973 (2008).

51. A Iguchi-Manaka, H Kai, Y Yamashita, K Shibata, S Tahara-Hanaoka, S i Honda, T Yasui, H Kikutani, K Shibuya, and A Shibuya. Accelerated tumor growth in mice deficient in DNAM-1 receptor. *Journal of Experimental Medicine* **205,** 2959–2964 (2008).

52. S E Street, E Cretney, and M J Smyth. Perforin and interferon-gamma activities independently control tumor initiation, growth, and metastasis. *Blood* **97,** 192–197 (2001).

53. M E van den Broek, D Kägi, F Ossendorp, R Toes, S Vamvakas, W K Lutz, C J Melief, R M Zinkernagel, and H Hengartner. Decreased tumor surveillance in perforin-deficient mice. *The Journal of experimental medicine* **184,** 1781–1790 (1996).

54. Erika Cretney, Kazuyoshi Takeda, Hideo Yagita, Moira Glaccum, Jacques J Peschon, and Mark J Smyth. Increased susceptibility to tumor initiation and metastasis in TNF-related apoptosis-inducing ligand-deficient mice. *J. Immunol.* **168,** 1356–1361 (2002).

55. M J Smyth, K Y Thia, S E Street, E Cretney, J A Trapani, M Taniguchi, T Kawano, S B Pelikan, N Y Crowe, and D I Godfrey. Differential tumor surveillance by natural killer (NK) and NKT cells. *The Journal of experimental medicine* **191,** 661–668 (2000).

56. Siddhartha Jaiswal, Catriona H M Jamieson, Wendy W Pang, Christopher Y Park,

Mark P Chao, Ravindra Majeti, David Traver, Nico van Rooijen, and Irving L Weissman. CD47 Is Upregulated on Circulating Hematopoietic Stem Cells and Leukemia Cells to Avoid Phagocytosis. *Cell* **138,** 271–285 (2009).

57. Ravindra Majeti, Mark P Chao, Ash A Alizadeh, Wendy W Pang, Siddhartha Jaiswal, Kenneth D Gibbs Jr, Nico van Rooijen, and Irving L Weissman. CD47 Is an Adverse Prognostic Factor and Therapeutic Antibody Target on Human Acute Myeloid Leukemia Stem Cells. *Cell* **138,** 286–299 (2009).

58. M P Chao, S Jaiswal, R Weissman-Tsukamoto, A A Alizadeh, A J Gentles, J Volkmer, K Weiskopf, S B Willingham, T Raveh, C Y Park, R Majeti, and I L Weissman. Calreticulin Is the Dominant Pro-Phagocytic Signal on Multiple Human Cancers and Is Counterbalanced by CD47. *Science Translational Medicine* **2,** 63ra94–63ra94 (2010).

59. Raghavan, M., Wijeyesakere, S. J., Peters, L. R. & Del Cid, N. Calreticulin in the immune system: ins and outs. *Trends in immunology* 1–9 (2012).

60. M Terme, E Ullrich, L Aymeric, K Meinhardt, M Desbois, N Delahaye, S Viaud, B Ryffel, H Yagita, G Kaplanski, A Prevost-Blondel, M Kato, J L Schultze, E Tartour, G Kroemer, N Chaput, and L Zitvogel. IL-18 Induces PD-1-Dependent Immunosuppression in Cancer. *Cancer Research* **71,** 5393–5399 (2011).

61. Diefenbach, A., Jensen, E., Jamieson, A. & Raulet, D. Rae1 and H60 ligands of the NKG2D receptor stimulate tumour immunity. *Nature* **413,** 165–171 (2001).

62. Robert Saddawi-Konefka, Timothy O'Sullivan, William Vermi, Catherine M Koebel, Cora Arthur, J Michael White, Ravi Uppaluri, Daniel M Andrews, Shin Foong Ngiow, Michele W L Teng, Mark J Smyth, Robert D Schreiber, and Jack D Bui. Cancer immunoediting by the innate immune system in the absence of adaptive immunity. *Journal of Experimental Medicine* **209,** 1869–1882 (2012).

63. Vladimir Ramirez-Carrozzi, Arivazhagan Sambandam, Elizabeth Luis, Zhongua Lin, Surinder Jeet, Justin Lesch, Jason Hackney, Janice Kim, Meijuan Zhou, Joyce Lai, Zora Modrusan, Tao Sai, Wyne Lee, Min Xu, Patrick Caplazi, Lauri Diehl, Jason de Voss, Mercedesz Balazs, Lino Gonzalez, Harinder Singh, Wenjun Ouyang, and Rajita Pappu. IL-17C regulates the innate immune function of epithelial cells in an autocrine manner. *Nature Publishing Group* 1–9 (2011).

64. Kawai, T. & Akira, S. Innate immune recognition of viral infection. *Nat Immunol* (2006).

65. Dranoff, G. Cytokines in cancer pathogenesis and cancer therapy. *Nature Reviews Cancer* **4,** 11–22 (2004).

66. Hirokazu Matsushita, Matthew D Vesely, Daniel C Koboldt, Charles G Rickert, Ravindra Uppaluri, Vincent J Magrini, Cora D Arthur, J Michael White, Yee-Shiuan Chen, Lauren K Shea, Jasreet Hundal, Michael C Wendl, Ryan Demeter, Todd Wylie, James P Allison, Mark J Smyth, Lloyd J Old, Elaine R Mardis, and Robert D Schreiber. Cancer exome analysis reveals a T-cell-dependent mechanism of cancer immunoediting. *Nature* **482,** 400–404 (2012).

67. Ma, Q. Role of Nrf2 in Oxidative Stress and Toxicity. *Annu. Rev. Pharmacol. Toxicol.* **53,** 401–426 (2013).

68. D Malhotra, E Portales-Casamar, A Singh, S Srivastava, D Arenillas, C Happel, C Shyr, N Wakabayashi, T W Kensler, W W Wasserman, and S Biswal. Global mapping of binding sites for Nrf2 identifies novel targets in cell survival response through ChIP-Seq profiling and network analysis. *Nucleic Acids Research* **38,** 5718–5734 (2010).

69. Dénes Türei, Diána Papp, Dávid Fazekas, László Földvári-Nagy, Dezső Módos, Katalin Lenti, Péter Csermely, and Tamás Korcsmáros. NRF2-ome: An Integrated Web Resource to Discover Protein Interaction and Regulatory Networks of NRF2. *Oxidative Medicine and Cellular Longevity* **2013,** 1–9 (2013).

70. K Yoh, K Itoh, A Enomoto, A Hirayama, N Yamaguchi, M Kobayashi, N Morito, A Koyama, M Yamamoto, and S Takahashi. Nrf2-deficient female mice develop lupus-like autoimmune nephritis. *Kidney Int.* **60,** 1343–1353 (2001).

71. Lee, J.-M., Chan, K., Kan, Y. W. & Johnson, J. A. Targeted disruption of Nrf2 causes regenerative immune-mediated hemolytic anemia. *Proceedings of the National Academy of Sciences of the United States of America* **101,** 9751–9756 (2004).

72. R A Linker, D H Lee, S Ryan, A M van Dam, R Conrad, P Bista, W Zeng, X Hronowsky, A Buko, S Chollate, G Ellrichmann, W Bruck, K Dawson, S Goelz, S Wiese, R H Scannevin, M Lukashev, and R Gold. Fumaric acid esters exert neuroprotective effects in neuroinflammation via activation of the Nrf2 antioxidant pathway. *Brain* **134,** 678–692 (2011).

73. Huanying Shi, Xu Jing, Xinbing Wei, Ruth G Perez, Manru Ren, Xiumei Zhang, and Haiyan Lou. S-allyl cysteine activates the Nrf2-dependent antioxidant response and protects neurons against ischemic injury in vitroand in vivo. *J. Neurochem.* n/a–n/a (2015).

74. Ann F Hubbs, Stanley A Benkovic, Diane B Miller, James P O'Callaghan, Lori Battelli, Diane Schwegler-Berry, and Qiang Ma. Vacuolar Leukoencephalopathy with Widespread Astrogliosis in Mice Lacking TranscriptionFactor Nrf2. *The*

American Journal of Pathology **170,** 2068–2076 (2010).

75. Copple, I. M., Goldring, C. E., Kitteringham, N. R. & Park, B. K. The Nrf2–Keap1 defence pathway: Role in protection against drug-induced toxicity. *Toxicology* **246,** 24–33 (2008).

76. Hybertson, B. M. & Gao, B. Role of the Nrf2 signaling system in health and disease. *Clin Genet* **86,** 447–452 (2014).

77. Magesh, S., Chen, Y. & Hu, L. Small Molecule Modulators of Keap1-Nrf2-ARE Pathway as Potential Preventive and Therapeutic Agents. *Med. Res. Rev.* **32,** 687–726 (2012).

78. Kensler, T. W. & Wakabayashi, N. Nrf2: friend or foe for chemoprevention? *Carcinogenesis* **31,** 90–99 (2010).

79. Kansanen, E., Kuosmanen, S. M., Leinonen, H. & Levonen, A.-L. The Keap1-Nrf2 pathway: Mechanisms of activation and dysregulation in cancer. *Redox Biology* **1,** 45–49 (1AD).

80. Jaramillo, M. C. & Zhang, D. D. The emerging role of the Nrf2-Keap1 signaling pathway in cancer. *Genes & development* **27,** 2179–2191 (2013).

81. Nguyen, T., Sherratt, P. J. & Pickett, C. B. REGULATORY MECHANISMS CONTROLLING GENE EXPRESSION MEDIATED BY THE ANTIOXIDANT RESPONSE ELEMENT. *Annu. Rev. Pharmacol. Toxicol.* **43,** 233–260 (2003).

82. Pablo E Pergola, Philip Raskin, Robert D Toto, Colin J Meyer, J Warren Huff, Eric B Grossman, Melissa Krauth, Stacey Ruiz, Paul Audhya, Heidi Christ-Schmidt, Janet Wittes, and David G Warnock. Bardoxolone Methyl and Kidney Function in CKD with Type 2 Diabetes. *New England Journal of Medicine* **365,** 327–336 (2011).

83. Tkachev, V. O., Menshchikova, E. B. & Zenkov, N. K. Mechanism of the Nrf2/Keap1/ARE signaling system. *Biochemistry Moscow* **76,** 407–422 (2011).

84. Timothy O'Sullivan, Robert Saddawi-Konefka, Emilie Gross, Miller Tran, Stephen P Mayfield, Hiroaki Ikeda, and Jack D Bui. Interleukin-17D Mediates Tumor Rejection through Recruitment of Natural Killer Cells. *CellReports* **7,** 989–998 (2014).

85. Saddawi-Konefka, R., O'Sullivan, T., Gross, E. T., Washington, A., Jr & Bui, J. D. Tumor-expressed IL-17D recruits NK cells to reject tumors. *oncoimmunology* **3,** e954853 (2015).

86. Wang, X. J., Hayes, J. D., Henderson, C. J. & Wolf, C. R. Identification of retinoic acid as an inhibitor of transcription factor Nrf2 through activation of retinoic acid receptor alpha. *PNAS* **104,** 19589–19594 (2007).

87. Ji Hee Moon, Ji-Sun Shin, Jong-Bin Kim, Nam-In Baek, Young-Wuk Cho, Yong Sup Lee, Hee Yeon Kay, Soo-dong Kim, and Kyung-Tae Lee. Food and Chemical Toxicology. *Food and Chemical Toxicology* **62,** 159–166 (2013).

88. Burshtyn, D. N. NK cells and poxvirus infection. *Front Immunol* **4,** 7 (2013).

89. Lanier, L. L. Evolutionary struggles between NK cells and viruses. *Nature Publishing Group* **8,** 259–268 (2008).

90. Matthias Schäfer, Hany Farwanah, Ann-Helen Willrodt, Aaron J Huebner, Konrad Sandhoff, Dennis Roop, Daniel Hohl, Wilhelm Bloch, and Sabine Werner. Nrf2 links epidermal barrier function with antioxidant defense. *EMBO Mol Med* **4,** 364–379 (2012).

91. Sporn, M. B. & Liby, K. T. NRF2 and cancer: the good, the bad and the importance of context. *Nature Reviews Cancer* **12,** 564–571 (2012).

92. Xiang, M., Namani, A., Wu, S. & Wang, X. Nrf2: bane or blessing in cancer? *J Cancer Res Clin Oncol* **140,** 1251–1259 (2014).

93. Akaike, T. Role of free radicals in viral pathogenesis and mutation. *Rev. Med. Virol.* **11,** 87–101 (2001).

94. Deramaudt, T. B., Dill, C. & Bonay, M. Regulation of oxidative stress by Nrf2 in the pathophysiology of infectious diseases. *Medecine et Maladies Infectieuses* **43,** 100–107 (2013).

95. L D Shultz, B L Lyons, L M Burzenski, B Gott, X Chen, S Chaleff, M Kotb, S D Gillies, M King, J Mangada, D L Greiner, and R Handgretinger. Human Lymphoid and Myeloid Cell Development in NOD/LtSz-scid IL2R null Mice Engrafted with Mobilized Human Hemopoietic Stem Cells. *The Journal of Immunology* **174,** 6477–6489 (2005).

96. Ma, Q. & He, X. Molecular Basis of Electrophilic and Oxidative Defense: Promises and Perils of Nrf2. *Pharmacological reviews* **64,** 1055–1081 (2012).

97. Yuanxiang Jin, Wenyu Miao, Xiaojian Lin, Xiuhong Pan, Yang Ye, Minjie Xu, and Zhengwei Fu. Acute exposure to 3-methylcholanthrene induces hepatic oxidative stress via activation of the Nrf2/ARE signaling pathway in mice. *Environ. Toxicol.* **29,** 1399–1408 (2013).

98. Gina M DeNicola, Florian A Karreth, Timothy J Humpton, Aarthi Gopinathan, Cong Wei, Kristopher Frese, Dipti Mangal, Kenneth H Yu, Charles J Yeo, Eric S Calhoun, Francesca Scrimieri, Jordan M Winter, Ralph H Hruban, Christine Iacobuzio-Donahue, Scott E Kern, Ian A Blair, and David A Tuveson. Oncogene-induced Nrf2 transcription promotes ROS detoxification and tumorigenesis. *Nature* **475,** 106–109 (2011).

99. Shelton, P. & Jaiswal, A. K. The transcription factor NF-E2-related Factor 2 (Nrf2): a protooncogene? *The FASEB Journal* **27,** 414–423 (2013).

100. Satoh, H., Moriguchi, T., Takai, J., Ebina, M. & Yamamoto, M. Nrf2 Prevents Initiation but Accelerates Progression through the Kras Signaling Pathway during Lung Carcinogenesis. *Cancer Research* **73,** 4158–4168 (2013).

101. Gu, C., Wu, L. & Li, X. IL-17 family: Cytokines, receptors and signaling. *Cytokine* **64,** 477–485 (2013).

102. Jin, W. & Dong, C. IL-17 cytokines in immunity and inflammation. *Emerging Microbes & Infections* **2,** e60 (2013).

103. Iwakura, Y., Ishigame, H., Saijo, S. & Nakae, S. Functional Specialization of Interleukin-17 Family Members. *Immunity* **34,** 149–162 (2011).

104. Gaffen, S. L. Recent advances in the IL-17 cytokine family. *Current opinion in immunology* **23,** 613–619 (2011).

105. Oberley, L. W. Free radicals and diabetes. *Free Radic. Biol. Med.* **5,** 113–124 (1988).

106. Szatrowski, T. P. & Nathan, C. F. Production of large amounts of hydrogen peroxide by human tumor cells. *Cancer Research* **51,** 794–798 (1991).

107. Y A Suh, R S Arnold, B Lassegue, J Shi, X Xu, D Sorescu, A B Chung, K K Griendling, and J D Lambeth. Cell transformation by the superoxide-generating oxidase Mox1. *Nature* **401,** 79–82 (1999).

108. Trachootham, D., Alexandre, J. & Huang, P. Targeting cancer cells byROS-mediated mechanisms:a radical therapeutic approach? *Nat Rev Drug Discov* **8,** 579–591 (2009).

109. Conner, D. A. Mouse embryo fibroblast (MEF) feeder cell preparation. *Curr Protoc Mol Biol* **Chapter 23,** Unit 23.2 (2001).

110. M Schafer, A H Willrodt, S Kurinna, A S Link, H Farwanah, A Geusau, F Gruber, O Sorg, A J Huebner, D R Roop, K Sandhoff, J H Saurat, E Tschachler,

M R Schneider, L Langbein, W Bloch, H D Beer, and S Werner. Activation of Nrf2 in keratinocytes causes chloracne (MADISH)-like skin disease in mice. *EMBO Mol Med* **6,** 442–457 (2014).

111. Fujita, K.-I., Maeda, D., Xiao, Q. & Srinivasula, S. M. Nrf2-mediated induction of p62 controls Toll-like receptor-4–driven aggresome-like induced structure formation and autophagic degradation. *Proceedings of the National Academy of Sciences of the United States of America* **108,** 1427–1432 (2011).